THE UNIVERSITY OF ADELAIDE

Examination of the Aeromagnetic Anomaly over the Talisker Mine areaon the southern Fleurieu Peninsula, South Australia.

by LESLIE HARVEY B.Sc. B.Sc. (Ma)

November, 1989

Examination of an Aeromagnetic Anomaly Over the Talisker Mine Area on the Southern Fleurieu Peninsula, South Australia.

by

Leslie M. Harvey, B.Sc., B.Sc.(Ma.)

This thesis is submitted in partial fulfilment of the requirements for the Bachelor of Science, Honours Degree (Geophysics) at the University of Adelaide.

November, 1989.

University of Adelaide,
Department of Geology and Geophysics.

CONTENTS

ACKNOWLEDGEMENTS

I wish to thank Professor David Boyd for introducing me to this most interesting and challenging project and for his role as supervisor. I also wish to thank my fellow honours students who have lent great support and motivation to me throughout the year.

I would especially like to thank Dr. Peter Brooker who has given me much guidance and reassurance throughout the year, and also Dr. Pat James for taking over in a supervisory role late in the year while Prof. Boyd was away.

Shanti Rajagopalan and Zhiqun Shi deserve special thanks for the many hours help each has given me. Finally, I would like to thank my family for their support and long sufferance throughout this difficult and challenging year.

ABSTRACT

A N-E striking elongate aeromagnetic anomaly is observed over the Talisker Mine area, on the Southern Fleurieu Peninsula, which has character and amplitude similar to an anomaly observed at Delamere (several kilometres to the north) found to be caused by magnetic Brachina Formation. Geological and geophysical techniques have been used to determine if the rock type at Talisker is also magnetic Brachina Formation, why there is a gap between the two anomalies, and why the anomaly at Talisker ends near the south coast.

Geological mapping, microscopy and petrologic studies have been used in conjunction with local ground magnetic surveys and modelling procedures, to reveal magnetic Brachina Formation as the cause of the anomaly at Talisker. Mapping has shown the anomaly to be the result of a sliver of magnetic Brachina Formation caught up within a local zone of intense deformation that extends for at least 1500m across strike, and which outcrops on the coast. The Brachina Formation is sheared out against Cambrian Backstairs Passage Formation to the south, forming the Southern end to the anomaly. To the north, the Brachina Formation suffered deeper erosion during Permian times, and is covered by a greater thickness of non-magnetic cover which causes the apparent gap in the aeromagnetic anomaly.

LIST OF FIGURES

CHAPTER 1: INTRODUCTION

The Ulupa Siltstone outcrops well in Stockyard Creek at Delamere and poorly in the Mt. Barker and Macclesfield areas (Fig. 1). All these areas correlate with strong aeromagnetic anomalies that appear to be continuous for strike extents of 5-10 km. An elongate aeromagnetic anomaly of similar character and amplitude is seen over the Talisker mine and the area south to the coast, near Cape Jervis on the Southern Fleurieu Peninsula (Fig. 2). This area is approximately 10 km south along strike from that showing the anomaly at Stockyard creek near Delamere, and will be referred to as the Talisker area. There is a separation between the anomalies that correlates with the Permian glacial cover seen in the area and is associated with deeper erosion (Fig. 3). The anomaly is elongate, extending approximately four kilometres in a N-NE direction from the south coast, with a width of less than one kilometre on the aeromagnetic data. The anomaly ends close to the coast south of the Talisker Mine site. Since the rocks in the Talisker area are predominantly of the Kanmantoo Group, it was suggested at the beginning of this study that examination of this anomaly may be a useful aid to mapping in the area.

The aim of this project is four-fold. To determine:

1. Whether this anomaly at Talisker is also produced by Ulupa Siltstone as in Stockyard creek, which was the suggestion of Mancktelow (1979),
2. Why the gap is present between the two anomalies,
3. Why the anomaly ends near the coast, and
4. To deduce the morphology, location, and orientation of the bodies creating the anomaly.

To resolve these problems, minor geological mapping was conducted in the Talisker area to locate the rock type responsible for the anomaly. The aeromagnetic data were used to obtain the regional details, while ground magnetic traverses were carried out to better delineate the anomaly, and then modelled to determine morphology and location of the magnetic bodies creating the anomaly.

Petrology was carried out in conjunction with modelling of the magnetic traverses, to determine whether the rock mineralogy and magnetic properties were consistent with values expected if Ulupa Siltstone was the cause of the magnetic anomaly at Talisker.

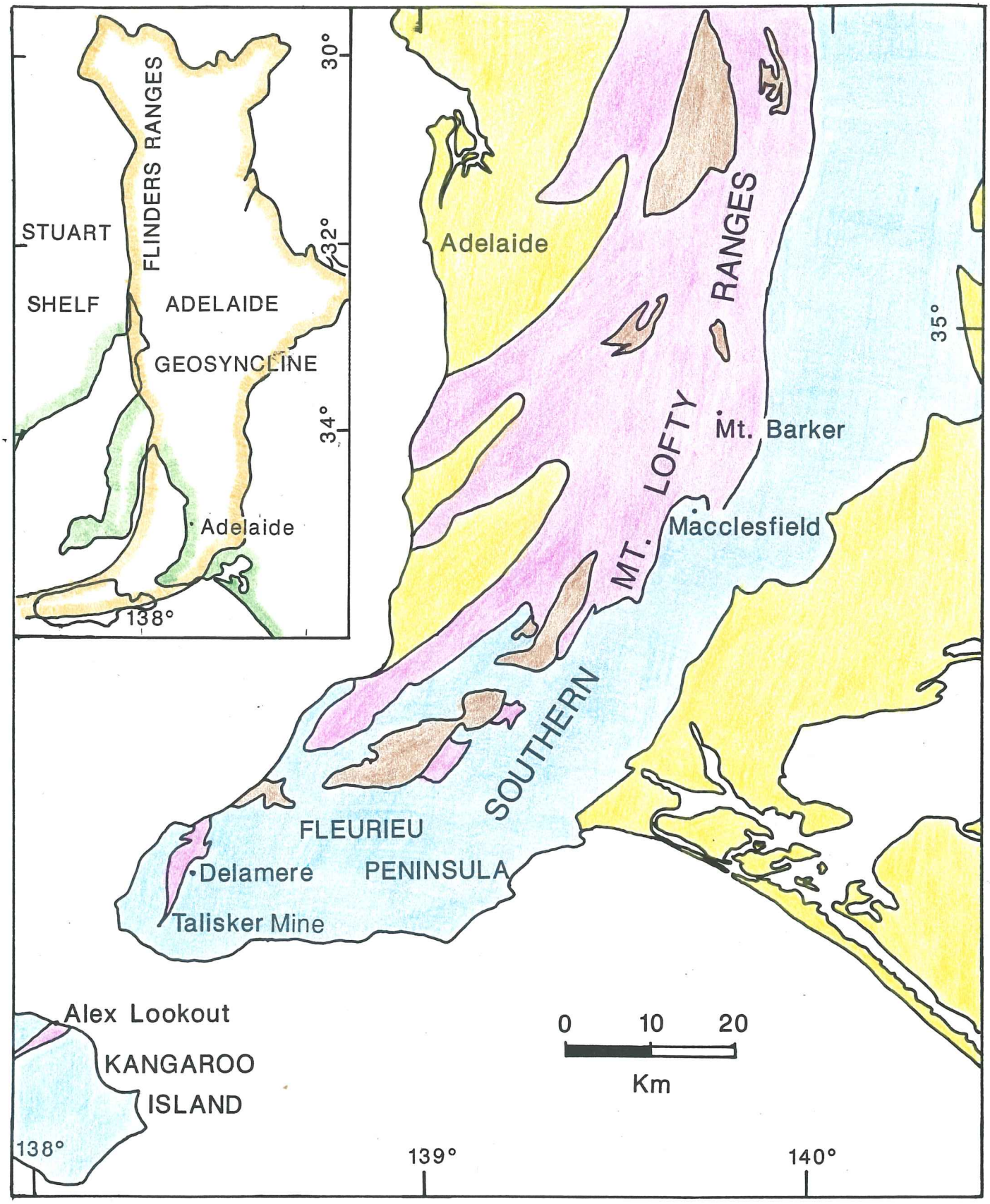

Figure 1: Locality Map

Figure 2: Contour map of Aeromagnetic data total magnetic field with overlay showing flightline positions and coastline.

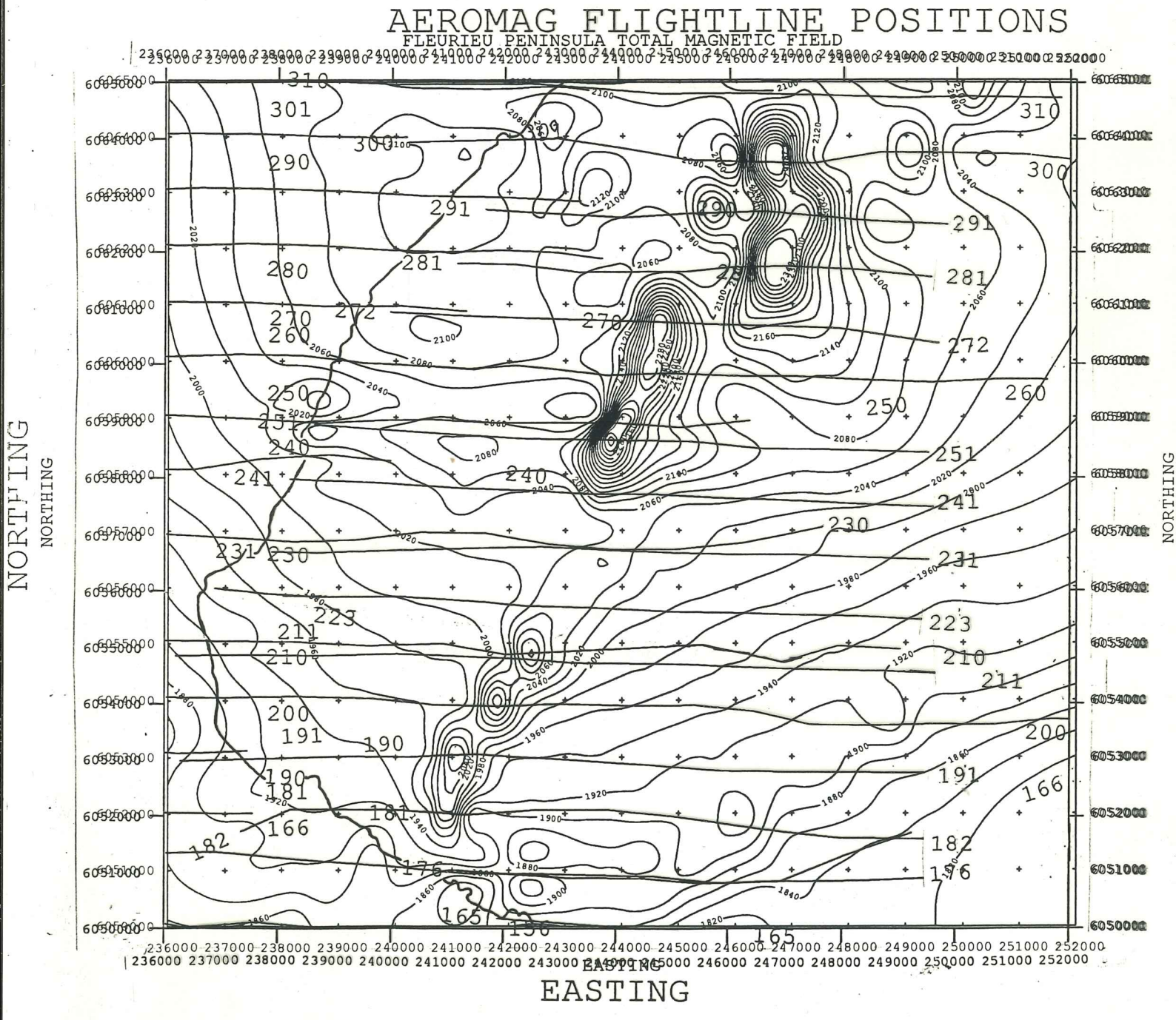

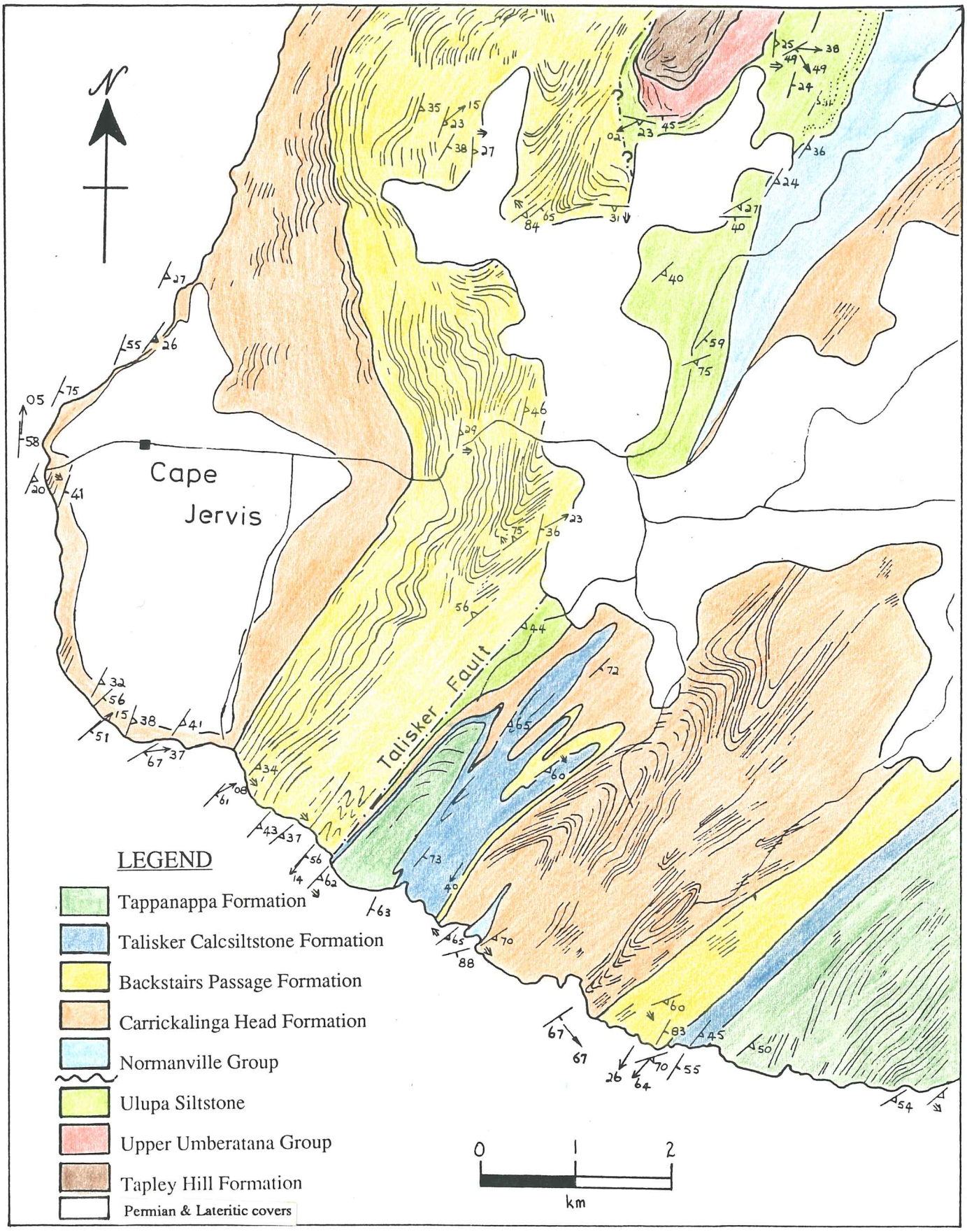

Figure 3: Geological map of Southern Fleurieu Peninsula (After Mancktelow 1979).

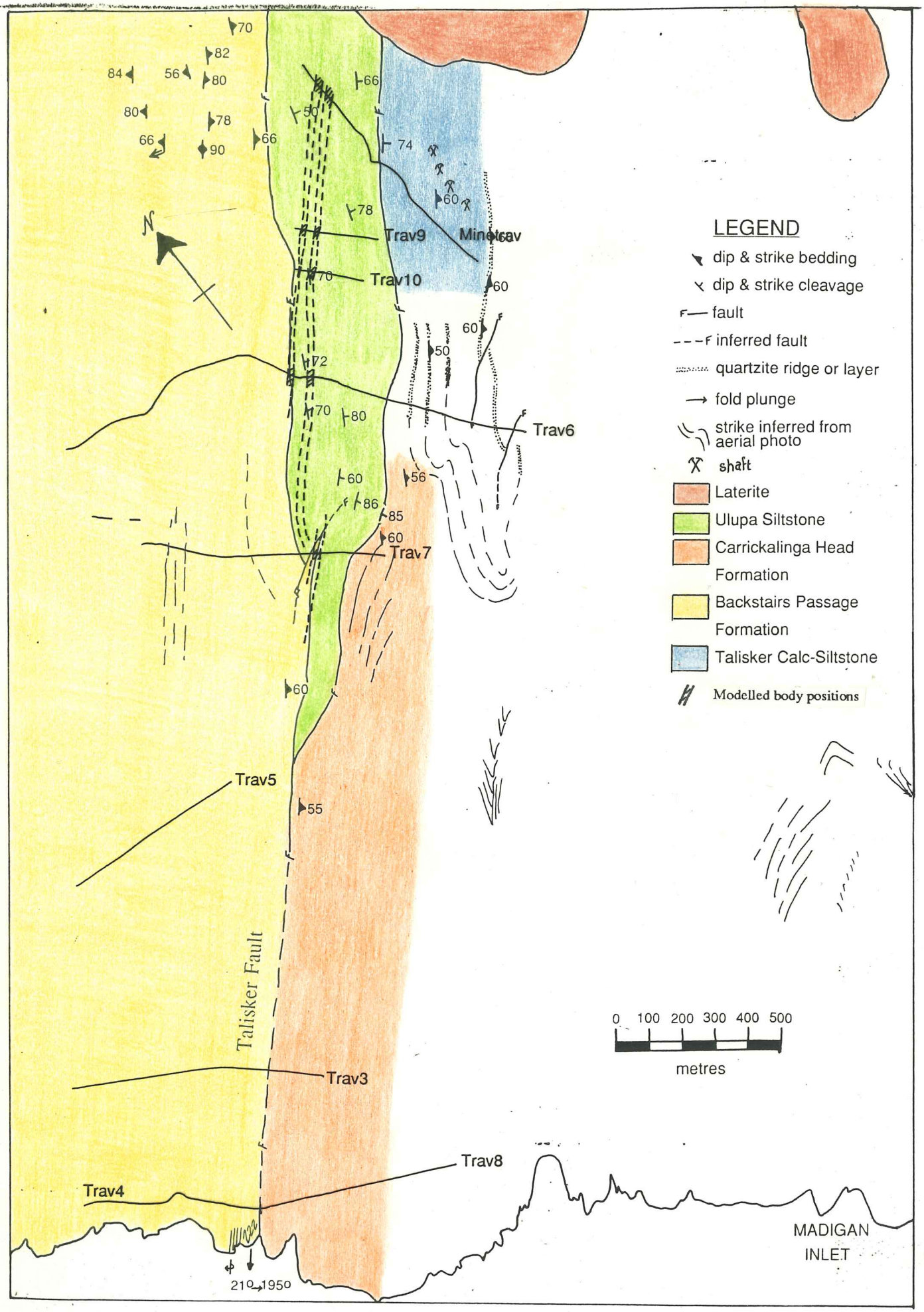

Figure 4: Geological map of Talisker area. Overlay shows positions of ground magnetic traverses and positions of modelled magnetic bodies.

CHAPTER 2: REGIONAL AND LOCAL GEOLOGY

2.1:REGIONAL GEOLOGY

2.1.1:Stratigraphy

The basement rocks in the Mt. Lofty Ranges, known as the Barossa Complex, consist of high grade metamorphic rocks which have been affected by the Delamerian retrograde metamorphism and shearing (Preiss, 1987). This Upper Proterozoic metamorphic basement is found in five anticlinal core inliers in the Mt. Lofty Ranges arranged en-echelon along the western margin of the Adelaide Fold Belt (Fig. 1) and is overlain unconformably by the Burra Group of the Adelaidean Supergroup. The western margins of these inliers are often faulted. The Aldgate Sandstone, an immature, feldspathic sandstone, is the basal unit and the rocks increase in argillite-carbonate content up sequence (Preiss, 1987).

The Umberatana Group overlies the Burra Group and is characterised by a massive tillite, arkose and quartzite sequence overlain by a thick pile of laminated siltstone and shale with some stromatolitic carbonates. These, in turn, are overlain by a marine glacial sequence and non-marine red sandstones and siltstones.

The Wilpena Group is the top of the Adelaide Supergroup seen in the Mt. Lofty Ranges. This contains a sequence of shale, siltstone, limestones and quartzites. Plummer (1978) referred to the Brachina Subgroup as consisting of the basal Nuccaleena Formation, Brachina Formation and the ABC Range Quartzite. The Brachina Formation has since been subdivided by Preiss (1987) into Seacliff Sandstone, Hallett Arkose and Ulupa Siltstone (Fig. 5). The Ulupa Siltstone was considered by Preiss (pers. comm.) to be a distal facies variant of the Brachina Formation and probably constitutes the most widespread depositional unit of the Brachina Subgroup in the Adelaide Geosyncline. A permanently-submerged, relatively shallow water environment under oxidising conditions was inferred for the red slates of the Brachina Formation, whereas the green-coloured, reduced, fine-grained sediments of the Ulupa Siltstone were considered to reflect deeper water conditions (Preiss, op. cit.). Sprigg (*in* Jenkins 1986) compared tertiary flysch sediments to the Ulupa Siltstone sediments, indicating a possible interpretation of turbidity current deposition for this unit. Late Pre-Cambrian and early Cambrian stratigraphy is summarized in Figure 6.

The Ulupa Siltstone is the most magnetic unit below the Kanmantoo Group and is often associated with a strong magnetic anomaly (Rajagopalan, 1989). It is the facies of Brachina Subgroup outcropping on the Fleurieu Peninsula and is the rock unit referred to by Stolz (1985) as "Magnetic Brachina Formation". Subdivision of the Brachina Formation as described above is adopted here, and the term "Ulupa Siltstone" will be used to describe the green phyllitic siltstone described by other workers as Brachina Formation.

There is a major hiatus between the Precambrian and the Cambrian sequences on Southern Fleurieu Peninsula. The base of the Cambrian in South Australia is regarded as an erosional disconformity separating quartzites of the Wilpena Group from the overlying base of the Cambrian Normanville Group (Mancktelow, 1979), which is characterised by carbonate and phosphate-rich rocks.

The Normanville Group is overlain by rocks of the Kanmantoo Group, a non-fossiliferous sequence of metamorphosed arkoses, greywackes, pelitic and calcareous rocks, however, the nature of this contact is not known. A monotonous sequence of predominantly greywackes is often used to describe the Kanmantoo Group, but the main lithologies are metasandstones and metaphyllites with interbedded metashales and minor carbonates, and are summarized in Figure 6.

Difficulty in mapping is experienced due to the lack of fossils and distinctive marker beds in the Kanmantoo Group, and the very monotonous sequence, especially in areas of poor outcrop. Large scale lithological repetitions within the Kanmantoo sequence were observed and documented by Daily and Milnes (1971,1973). This lead to recent speculation (Jenkins, 1986; Steinhardt, in press) on the presence of a series of thrust faults along the south coast that may have repeated the stratigraphy, rather than the whole Kanmantoo Group being a single stratigraphic sequence. However, little field evidence has been presented to support this idea at this stage.

The best marker horizon in the Kanmantoo Group is the Talisker Calc-siltstone Formation which intertongues the Backstairs Passage Formation, and itself produces a prominent magnetic signature. The Kanmantoo Group conformably overlies the Normanville Group in the type section along the south coast.

Sedimentation in the Adelaide Geosyncline (Fig. 1) started in the late Proterozoic and continued into the early Palaeozoic (Both, in press). The Adelaidean sedimentary record is thin in the Southern Mt. Lofty Ranges, suggesting subsidence may have been less pronounced than in the Flinders Ranges. Evidence suggests the sedimentary basin collapsed soon after the initiation of Cambrian deposition resulting in the very rapid accumulation of dominantly flysch facies sediments of the Kanmantoo Group in the Southern Mt. Lofty Ranges, while steady subsidence in the Flinders Ranges developed shallower-water, shelf-facies, carbonates (Both, in press).

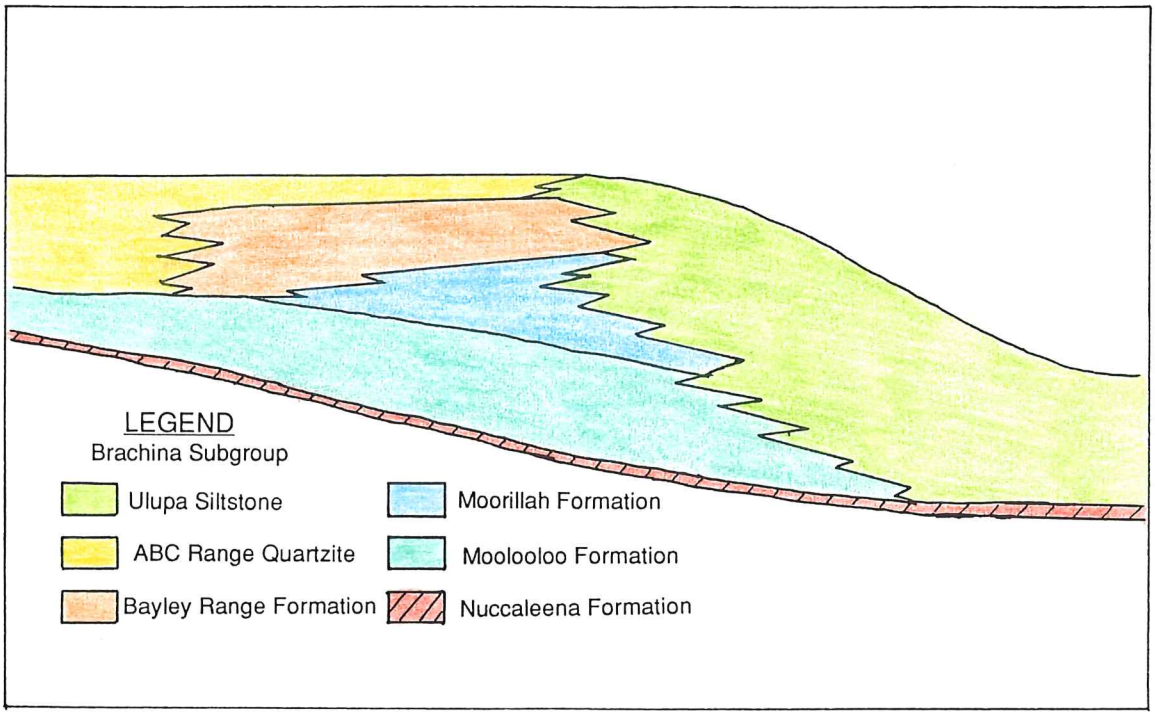

Figure 5: Rock relation diagram for the Brachina Subgroup showing the relationship of the Ulupa Siltstone to Brachina Subgroup.
(Modified from Plummer, 1978).

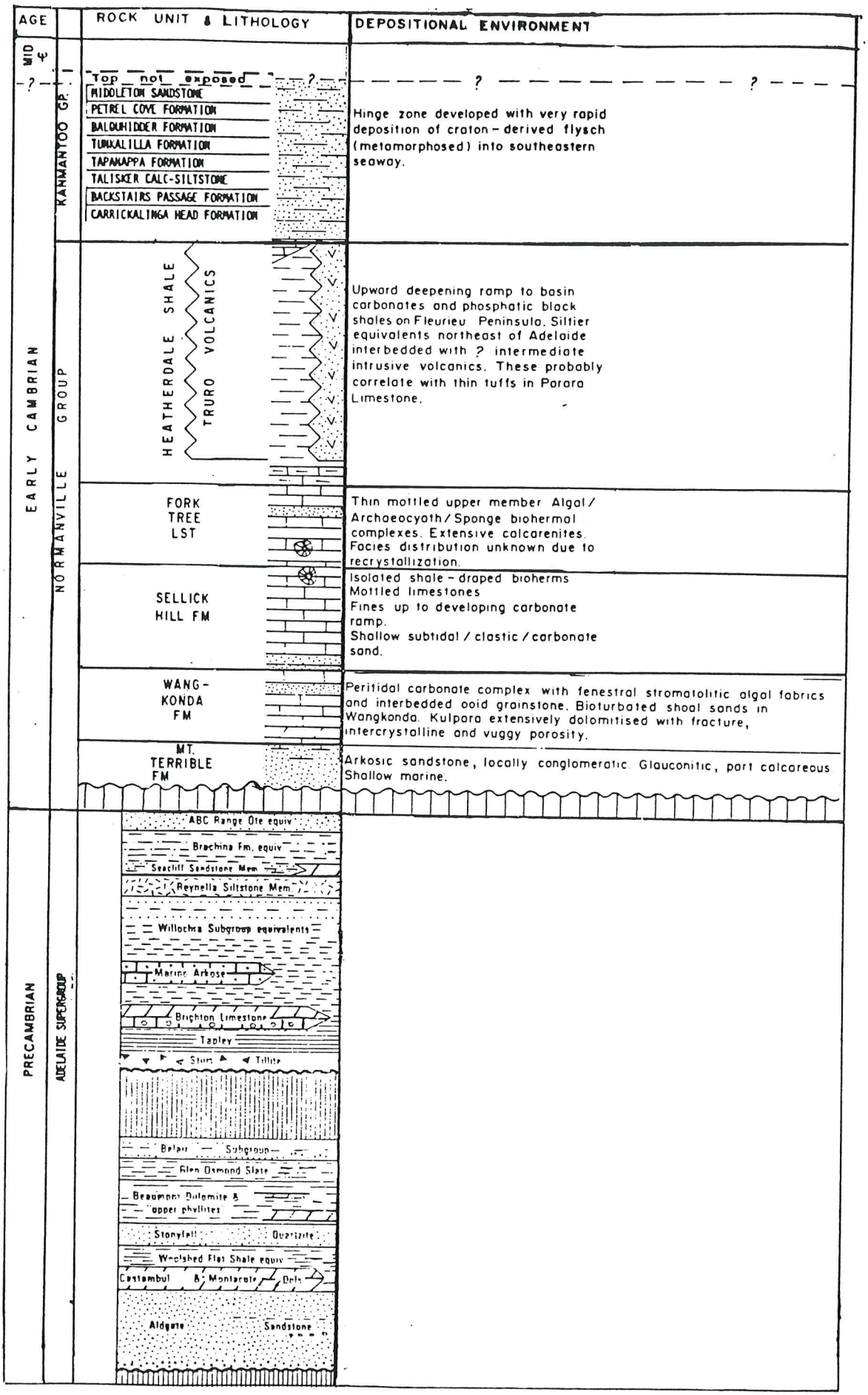

Figure 6: Stratigraphic Table of Upper Pre-Cambrian and Lower Cambrian. (Modified from Thomson et al, 1976; Dalgarno, 1983; SADME, 1989)

2.1.2:Structure

Kanmantoo Group sedimentation ceased in the middle to late Cambrian due to compressional tectonics associated with the Cambro-Ordovician Delamerian Orogeny (515-450 Ma) which caused variably intense deformation and metamorphism throughout the Adelaide Fold Belt (Fig. 1).

Five deformational events have been documented in the Kanmantoo Group rocks, of which Mancktelow (1979) considered only the early D_1 event (515-500 Ma) to be important in the Adelaide Fold Belt. F_1 folds in the Fleurieu Peninsula are generally upright with inclined to overturned, asymmetric folds with easterly dipping axial planes. The steep to overturned westerly limbs are thinned and have often developed into small thrust zones.

Mancktelow (1979) showed that five distinct zones of metamorphic grade exist in the Adelaide Fold Belt. The Talisker area has suffered upper greenschist facies metamorphism with mineral assemblages characteristic of low pressure, intermediate type metamorphism with pressures of 3-4 kb and temperatures of 650^{o}C (Offler and Fleming, 1968). Magnetic minerals could have formed during metamorphism with magnetite the main source of most magnetic anomalies (Rajagopalan, 1989).

2.2: Geological Mapping of the Talisker Area

Minor geological mapping was carried out in an elongate zone from the mine site at Talisker to the south coast in the vicinity of the magnetic anomaly, in order to identify the rock types producing the different magnetic responses (Fig. 4). Another aim was to locate the previously-mapped Talisker Fault, and the extent of the magnetic Ulupa Siltstone (Fig. 4) in the Talisker area. Campana and Wilson(1954), George (1963) and Mancktelow (1979) separately located the Talisker Fault, but this was generally mapped with little field evidence.

George (1963) did considerable mapping in the Talisker area. However, he failed to recognise Ulupa Siltstone and considered all the rock units in the area to belong to the Kanmantoo Group. He mapped the phyllites recognised here as the Ulupa Siltstone, to lie within the Nairne Formation Equivalent (now known as the Talisker Formation). George (op. cit.) failed, therefore, to recognise the importance of the Talisker Fault zone and hence mapped its position incorrectly.

The mapping conducted by the author (Fig. 4) shows Kanmantoo Group rocks are the predominant rock type outcropping in the area. A continuous sequence of weakly-deformed, southeasterly-dipping, Backstairs Passage Formation is seen in the westerly section of the map to the west of the Talisker Fault. The zone within 200m of the Talisker Fault becomes tightly folded (Fig. 4). These folds have shallowly-dipping eastern limbs with steep to overturned and thinned westerly limbs, with a constant gentle southerly plunge of their fold axes at 20° towards 195°, and have similar style to the macroscopic folds observed on the Fleurieu Peninsula (Fig 7a).

The Backstairs Passage Formation is sharply truncated at the previously-mapped Talisker Fault, which extends north past Delamere (Fig. 3). This fault represents the western margin of a major zone of intense deformation and shearing in the Talisker area. The eastward extent of this zone is unclear as it was not the subject of this study to determine the easterly extent. However, the intense deformation zone may extend eastwards at least as far as Madigan Inlet on the coast.

The zone of shearing contains minor isoclinal folds which have widely varying plunge directions. Shallow southerly plunges to steep northerly plunges were observed, and boudinaging was common (Fig. 7d). Upright axial planes also give way to inclined axial planes

a: Massive quartzites of the Backstairs Passage Formation to the west of the zone of shearing have similar style to the macroscopic folds on the Fleurieu Peninsula. The folds have gently dipping easterly limbs with steep to overturned westerly limbs and gentle southerly plunges.

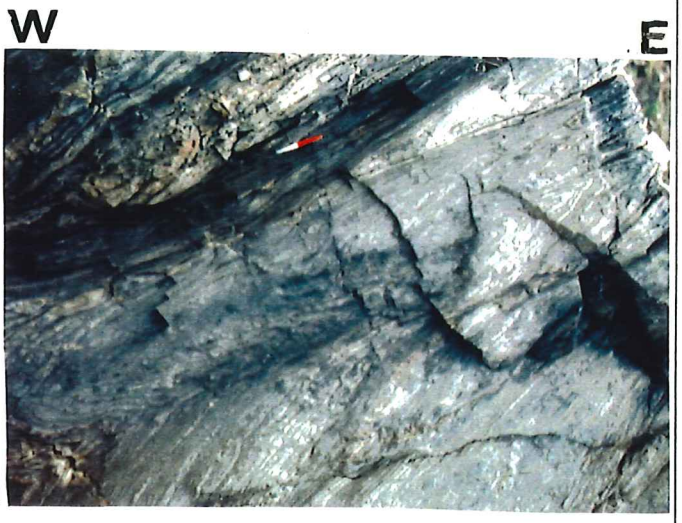

b: A common feature within the zone of shearing is small shears developed into minor local faults.

c: Competant layers show the highly varying fold plunges seen within the zone of shearing.

d: Boudinage is common within the zone of shearing.

Figure 7:

in the shear zone (Fig 7c). A prominant lineation with an orientation of 70° towards 115° is seen throughout and characterizes the zone of shearing, although a sense of movement was not determined. The zone is bedding-parallel to sub bedding-parallel and contains lenses of less-deformed rocks that dip steeply to the east. These lenses do not show the tight folding and lineation features of the highly-sheared phyllites and are generally coarser grained.

The oldest rocks present in the Talisker area were green phyllites of the Ulupa Siltstone. The phyllites are very fine-grained but contain single crystals of magnetite observable in hand specimen. The phyllites have a well developed cleavage which show this strong lineation. Mapping shows this to be a small tongue of Ulupa Siltstone that has become caught up in the zone of intense deformation, and is wedged between two blocks of thick Cambrian Kanmantoo Group sequence. To the south, the outcrop of the Ulupa Siltstone is eventually cut out against the Talisker Fault along the western margin of the shear zone at a position which correlates with the southern extent of the magnetic anomaly in the area (Fig. 4).

To the east of the Ulupa Siltstone lie grey phyllites of the Kanmantoo Sequence with thick interbeds of clean to muddy quartzites. These appear to belong to the Carrickalinga Head Formation from the lithologies observed, however, as previously mentioned, identification of these rock units is very difficult, and further mapping may prove this interpretation incorrect. These phyllites also develop the lineation and deformation features common in the shear zone, whilst the more competent quartzites appear relatively undeformed.

The rock unit observed at the Talisker Mine site itself (Talisker Calc-siltstone) has considerably more carbonate, which occurs as bands within generally muddy quartzites and phyllites. This unit also displays the highly-deformed nature of rocks within the shear zone with small scale isoclinal folding and highly-variable fold plunges being observed. The boundary between the Talisker Calc-siltstone Formation and the Carrickalinga Head Formation to the south was not determined, however the boundary is likely to be caused by one of the minor reverse faults that are commonly observed in the more competant quartz-rich layers (Fig. 4). These faults generally are parallel or subparallel to bedding and are not easily identified unless they cut one of the more prominent quartzite layers.

The juxtaposition of rock types, and the intense folding associated with the zone of shearing, suggests a compressional regime, and may be consistent with broad scale thrusting in the area.

CHAPTER 3: MAGNETICS

3.1:Rock Magnetism

There are several major physical properties which determine the magnetism of a rock unit, the most significant of which is susceptibility *K*. These are controlled by the abundance, composition and form of the magnetic mineral grains in the rock unit (Dobrin, 1981). The net magnetic response of a rock varies with the geological processes which affect the petrogenesis of the magnetic minerals.

Magnetic minerals in metasediments may be primary (depositional) or secondary (diagenetic and metamorphic), and the form and amount of iron in the sediments controls the production of magnetic minerals during metamorphism (Dobrin, 1981). Heavy minerals present in greywackes commonly include primary magnetite with ilmenite and rutile. During diagenesis, magnetite can be produced by the reduction of haematite or the oxidation of pyrite.

Magnetite is formed by the breakdown of (Mg,Fe) silicates at all grades of regional metamorphism and forms euhedral to subhedral porphyroblasts.

$$\text{Chlorite} \pm \text{Biotite} \pm \text{Haematite} \rightleftharpoons \text{Muscovite} \pm \text{Kfeldspar} + \text{Magnetite} + SiO_2 + H_2O.$$

(Stacey & Bunerjee, 1974)

Magnetic anomalies are caused by the bulk magnetism of rocks, which can be separated into two components.

1. Magnetization induced by the earth's field in the same direction as the present day induced magnetic field.

$B=KH$ where K=susceptibility .

H=strength of earth's field

=60,000 nT at Talisker .

2. Natural remnant magnetization (NRM) with intensity *J*.

This is the bar magnet effect of permanent magnetization and is independent of the present-day earth's field. This is usually acquired during a geological event or events such as metamorphism and cooling of igneous rocks to below the Curie temperature, where the field direction at that time becomes imprinted in the rock.

The resultant magnetization is the vector sum of these two components and is usually dominated by the induction component, as in the Talisker area. (See section 3.2)

Since the Earth's field strength is constant within a region, the susceptibility of a rock type will have a large effect on the size of the magnetic anomaly produced, and changes in susceptibility will have a direct impact on the anomaly shape and size.

3.2: Remnant Magnetization

Rajagopalan (1989) showed that the Ulupa Siltstone could possess significant remnant magnetization component which could affect the modelling of magnetic anomalies. Stolz (1985) found the Ulupa Siltstone at Delamere to have "a significant but not overwhelming effect on magnetic profiles modelled", having a remnant component with intensity 123nT in a direction similar to the Earth's present field (Declination: 40°; inclination:-64°).

Magnetite produces large induction effects and thus high magnetic susceptibilities in rocks especially when the magnetite grains are large (1% magnetite produces susceptibilities of the order of 3000×10^{-5}SI in unweathered rocks) whilst Titaniferous magnetite (magnetite/ulvospinel) may produce large NRM components in rocks. This, however, depends on the amount and the size of the grains, and large grains of this mineral association are required to produce large NRM components. Titaniferous magnetite is exsolved on cooling of the rocks from higher grade metamorphic conditions. Once the temperature falls below the Curie point for these minerals, the NRM is acquired and retained in the rock.

The mineral associations seen in the Ulupa Siltstone (see Chapter 5) show significant quantities (approx. 5%) of large porphyroblasts of magnetite, whilst titaniferous magnetite exists in small amounts (less than 1%) as fine grains. Hence, the overall remnant magnetization effect is expected to be low, with the magnetic response dominated by the induction effect in the Talisker area. Good correlation was produced between geological mapping and magnetic modelling, using only induction within the modelling, when negative susceptibilities are incorporated into the models. This indicates that the NRM component is significant, but the small magnitudes indicate it is not overwhelming within these models.

Remnance studies by Stolz (1985) and Rajagopalan (1989) suggested NRM in the Ulupa Siltstone formed during metamorphism and is chemical in origin.

The Ulupa Siltstone in the Talisker area is very weathered and poorly-outcropping. This makes it difficult to collect fresh samples for palaeomagnetic measurements. Weathered rocks produce very scattered palaeomagnetic direction measurements and hence, make poor targets for palaeomagnetic studies (F. Chamalaun pers. comm., 1989).

Due to the difficulty in collecting fresh samples at Talisker, palaeomagnetic analysis will not give sufficient clarity to determine an accurate direction and magnitude for NRM, and will not be attempted within this project.

3.3: Magnetic Susceptibility Measurement

Outcrop susceptibility measurements were made using a hand held Geoinstruments JH-8 susceptibility meter and are summarized in Table 1. Susceptibilities give a guide to the magnetic response induced in the sample and hence give a measure of the magnetic strength of the rock unit. The samples measured were all taken from exposed outcrop which had suffered considerable weathering. Some susceptibilities measured were lower than expected as a result of this weathering, and measured susceptibilities may not be representative of fresh rock susceptibilities. In particular, due to this weathering effect, the measured susceptibility values for the Ulupa Siltstone are all an order of magnitude lower than those measured in other areas by Rajagopalan (1989) and Stolz (1985), which averaged 1000×10^{-5} SI units. The measured susceptibilities are also lower than the susceptibilities required to produce an anomaly of this size as determined by modelling. However, Ulupa Siltstone susceptibilities are significantly higher than susceptibilities from the Kanmnatoo Group rocks (5×10^{-5}-15×10^{-5} SI) and indicate this is the most likely rock unit to produce the observed anomaly. These higher susceptibilities correlate with magnetic beds in the Ulupa Siltstone.

Examination of thin sections (see Chapter 5) reveals a martite texture in the magnetites caused by alteration of magnetite to haematite as a result of weathering. This accounts for the low susceptibilities measured in the hand samples.

SUSCEPTIBILITY MEASUREMENT OF HAND SAMPLES

Sample No.	Stratigraphic Group	Susceptibility (SI)
920-1a	Ulupa Siltstone	$10x10^{-5}$
920-1b	Ulupa Siltstone	$70x10^{-5}$
920-1c	Ulupa Siltstone	$83x10^{-5}$
920-1d	Ulupa Siltstone	$100x10^{-5}$
920-1e	Ulupa Siltstone	$100x10^{-5}$
920-1/16	Kanmantoo	$13x10^{-5}$
920-5/16	Kanmantoo	$10x10^{-5}$
920-1/24	Kanmantoo	$15x10^{-5}$
920-1/24	Kanmantoo	$12x10^{-5}$
920-3/24	Kanmantoo	$15x10^{-5}$
920-4/16	Kanmantoo	$2x10^{-5}$
920-2/24	Kanmantoo	$7x10^{-5}$
920-3/16	Kanmantoo	$5x10^{-5}$
920-7/16	Kanmantoo	$5x10^{-5}$
920-2/16	Laterite	$40x10^{-5}$
920-1/17	Laterite	$25x10^{-5}$
920-2/17	Laterite	$28x10^{-5}$
920-3/17	Laterite	$15x10^{-5}$

Table 1: Table of hand sample susceptibility measurements.

CHAPTER 4: GEOPHYSICAL FORWARD MODELLING

4.1: Modelling of Aeromagnetic Anomalies

An aeromagnetic survey was flown over the Southern Fleurieu Peninsula, Kangaroo Island and Southern Stansbury Basin in 1982 by Geoex Pty. Ltd., for the South Australian Department of Mines and Energy (SADME). Lines were flown east-west at 1 km spacings with tie lines every 5 km flown north-south. The survey produced the aeromagnetic data used for modelling in this project. A contour map of this data is seen in Figure 2. The data contains a strong regional gradient which needs to be removed for effective modelling because the presence of the broad gradient in the profile data makes it difficult to see when the model fits the data well. Analysis of the data has shown this to be produced by a body at a depth of 3-4km. Since the anomaly of interest is produced by a body at shallow depths, the deep body is not of interest in the present study and can be removed from the data.

A computer program which uses a least squares polynomial fit method (Residual2 ;R. Kennedy, 1989) was used to remove the regional gradient. The program was adapted to suit the Stansbury Basin data. A second degree polynomial regional curve produced a goodness of fit of 82.5% and gave a residual map with a relatively flat background gradient (Fig. 8). This was considered to be accurate enough for modelling purposes. Figure 9 shows the regional gradient removed by this program.

Modelling of the data was carried out using the two-dimensional forward modelling program GAMMA (Paine, 1985) which runs interactively on a microVAX/VMS 4.6 operating system. GAMMA allows data for dipping dyke, polygon, or slab-shaped bodies to be input for modelled magnetic bodies. A maximum of 15 bodies can be input for any one model. Due to the approximately isoclinal nature of the folds in the Talisker area, and the monoclinal, moderately-steep dip on the beds, dipping dyke-like bodies were generally used to represent the different magnetic and non-magnetic rock units and these correlated well with the observed geology. The local inclination, declination, and magnetic field intensity can be input into GAMMA and the model response calculated accordingly. GAMMA allows easting or northing lines to be input, and allows data to be input from the screen or from files.

Figure 8: Contour map of Residual Magnetic data after the removal of a second order polynomial from the original data. Overlay shows the positions of the Talisker and Delamere anomalies.

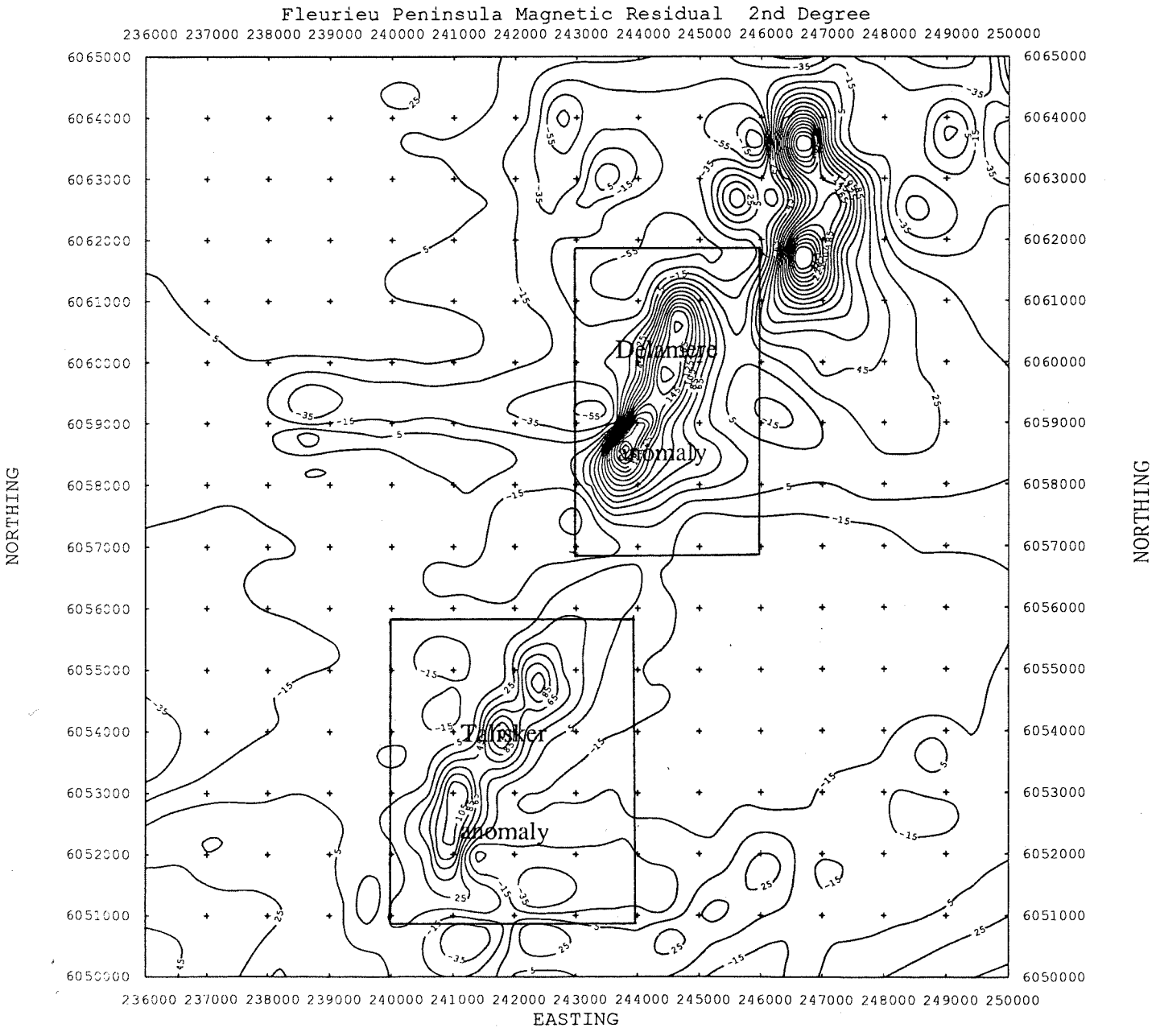

Figure 9: Contour map of second order polynomial removed as regional from original data.

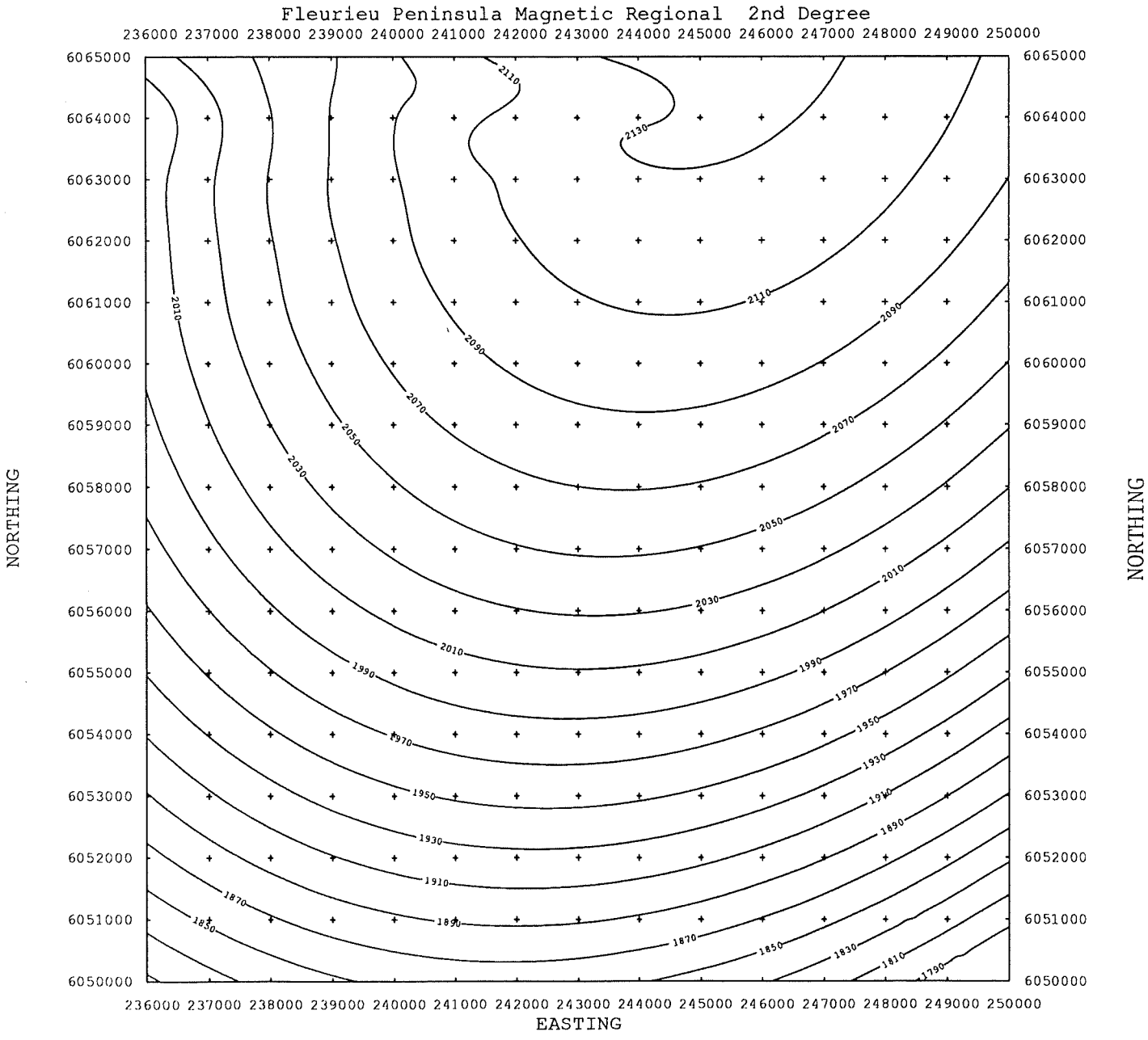

The variable parameters which were input into GAMMA include strike, dip, width, depth and depth extent, position on the profile, susceptibility, and NRM of the body. These parameters can all be input directly from the screen and are altered interactively. GAMMA enables both total field and vertical gradient field measurements to be analysed, and the data and model response are both plotted on the screen to enable easy comparison. The model is considered to be good when the model response curve shows a good fit with the vertical gradient curve and the total field curve. Variation in background levels can have a considerable effect on the total field curve, however, changes in background levels do not affect the vertical gradient curve. Vertical gradient also produces greater resolution of small anomalies, near surface anomalies, and gives the advantage that most of the regional field is removed. Hence, the primary tool used for modelling the data is the vertical gradient curve with the total field curve being used as a check to the accuracy of the model.

GAMMA is a two-dimensional modelling program which means that it assumes infinite strike extent perpendicular to the profile. (Readers are referred to Rajagopalan (1989, Chapter 4) for detailed mathematics utilised by GAMMA.) The assumption of infinite strike extent is reasonable when the body extends in both directions away from the profile, at least ten times the depth to the magnetic body. Hence, problems may occur when magnetic bodies end, as is seen with the Ulupa Siltstone in the Talisker area. (See Section 4.3 for discussion)

4.2: Correction of Profile Positions

Ground magnetic traverses revealed the position of peaks within the air-borne data to be incorrect. Up to 600m difference was observed between the position of anomaly peaks in the air-borne data to the position of peaks as determined by ground traverses. Due to the proximity of the ground magnetic traverses to the magnetic bodies and the fact that the assumptions of constant velocity and accurate aircraft positioning made in the air-borne data may be unjustified, the ground data is taken as correct. Errors in the air-borne data are introduced because positions of the aircraft are taken from aerial photographs. These are taken at regular intervals and a constant velocity assumed between locations. Errors develop when the velocity is not constant

between the two positions. Also, if the aircraft is not level, the photograph will not be taken directly below the aircraft, so adding further errors.

Ground profiles were carried out that corresponded closely to the position of the air-borne profiles. The error in the position of the air-borne profile was then calculated and the profiles adjusted by adding a constant shift to each data point in the profile. A contour map of the corrected data can be seen in Figure 10.

Figure 10: Contour map of aeromagnetic data after correction of the Talisker anomaly. Overlay shows area corrected using the ground magnetic data.

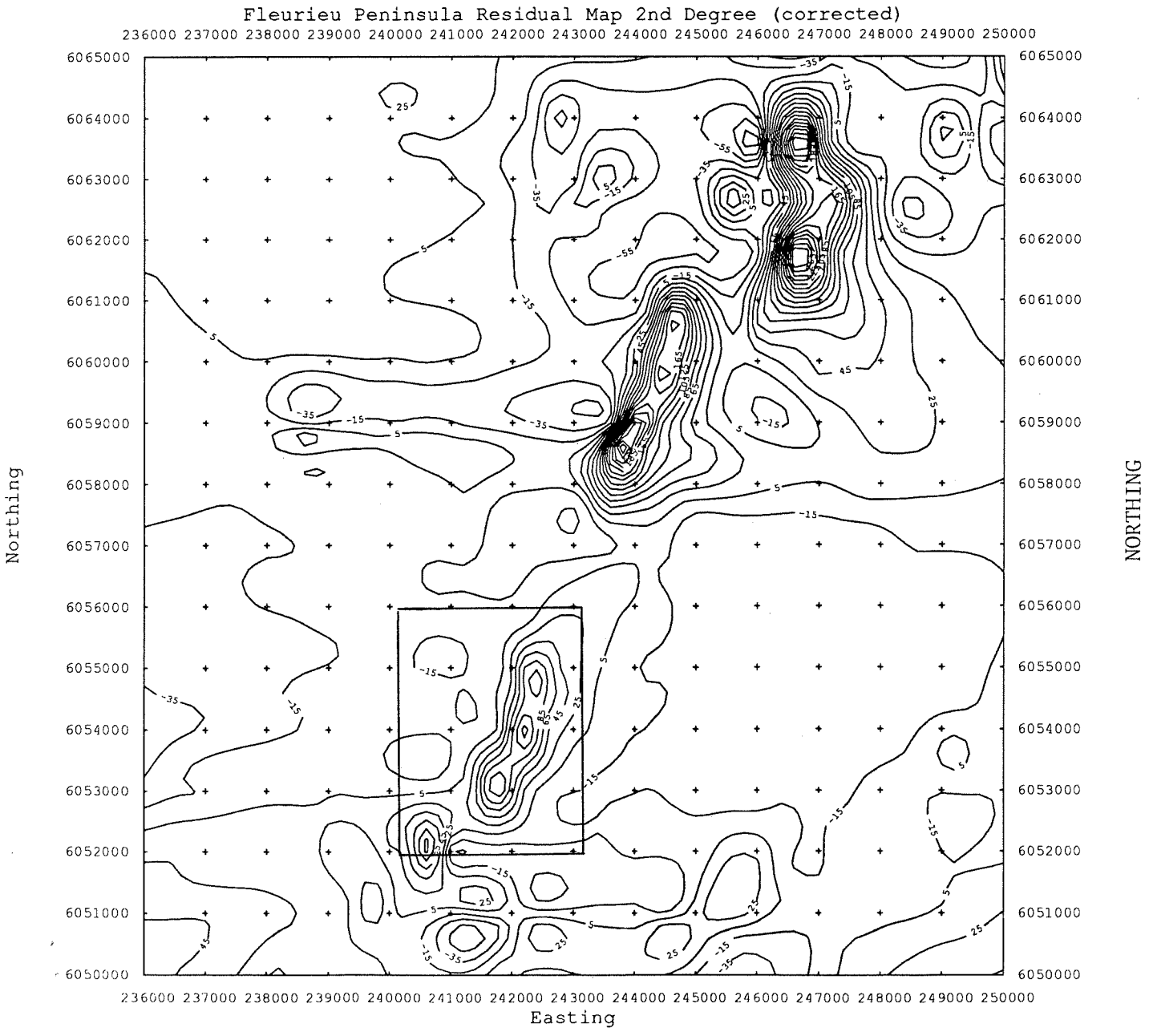

4.3: Discussion of Models

Aeromagnetic data profile lines 166, 182, 191, 200 and 223 were all modelled using Gamma and the residual data. Lines 200, 210 and 211 have very similar profiles and are considered to be produced by similar rock geometries, so all three lines are assumed to have the same model as line 200. The modelled lines with their associated models are presented in Figures 11 to 15. (Details of the bodies are presented in Appendix One)

Some bodies in the models were modelled with negative susceptibilities. Negative susceptibilities are not naturally observed in rock samples and imply the presence of NRM when incorporated into models. As well as this, ambiguity associated with magnetic forward modelling can produce negative susceptibilities within a model. If this profile is later remodelled with a similar model, negative susceptibilities may not be incorporated due to the slight variations in the model. So, negative susceptibilities are only an indication that an NRM component is present. It can be concluded therefore, that NRM in the Talisker area is significant but not overwhelming and the magnetic response is likely to be dominated by the induction effect.

The model responses do not always correspond to the regional value especially on the ends of lines. This could be due to the poor fit of the regional gradient polynomial at the edge of the data, or the effect of adjacent bodies not being modelled. Good fits to the vertical gradient data in these cases are accepted as good models. This only occurs at the edges of the profiles, away from the area of interest.

4.3.1: Line 166

The profile for line 166 shows a small amplitude peak, but with a large negative to the west. This can be modelled with a thin magnetic body corresponding to the Ulupa Siltstone next to a body with large negative susceptibility. Line 166 corresponds approximately to the position of the end of the magnetic Ulupa Siltstone outcrop as mapped (Fig. 4). Hence, the very different profile characteristics and corresponding model for this line are likely to be due to an end effect produced by the end of the body, and may not be representative of the true geometry of the underlying rock units. The assumption of infinite strike extent is not satisfied and so the model produced by Gamma cannot be assumed to be correct in the vicinity of the magnetic Ulupa Siltstone body.

The bodies modelled adjacent to the magnetic bodies were consistent with the observed geology and other models. Constantly dipping bodies were used to simulate the uniform dip generally observed in the area. The magnetic bodies are surrounded by relatively non-magnetic bodies with susceptibilities generally less than 10×10^{-5} SI units. These bodies correspond to the Kanmantoo Group rocks that generally have low susceptibilities. Small anomalies in the profile are modelled by thin bodies of slightly higher susceptibility. These represent layers within the Kanmantoo Group sequence with higher magnetic properties.

To the east, a large peak is observed and modelled by a body with moderately high susceptibility. This corresponds to the position of the Talisker Calc-siltstone beyond the shear zone which is considered to be a magnetic marker bed in the Kanmantoo Group.

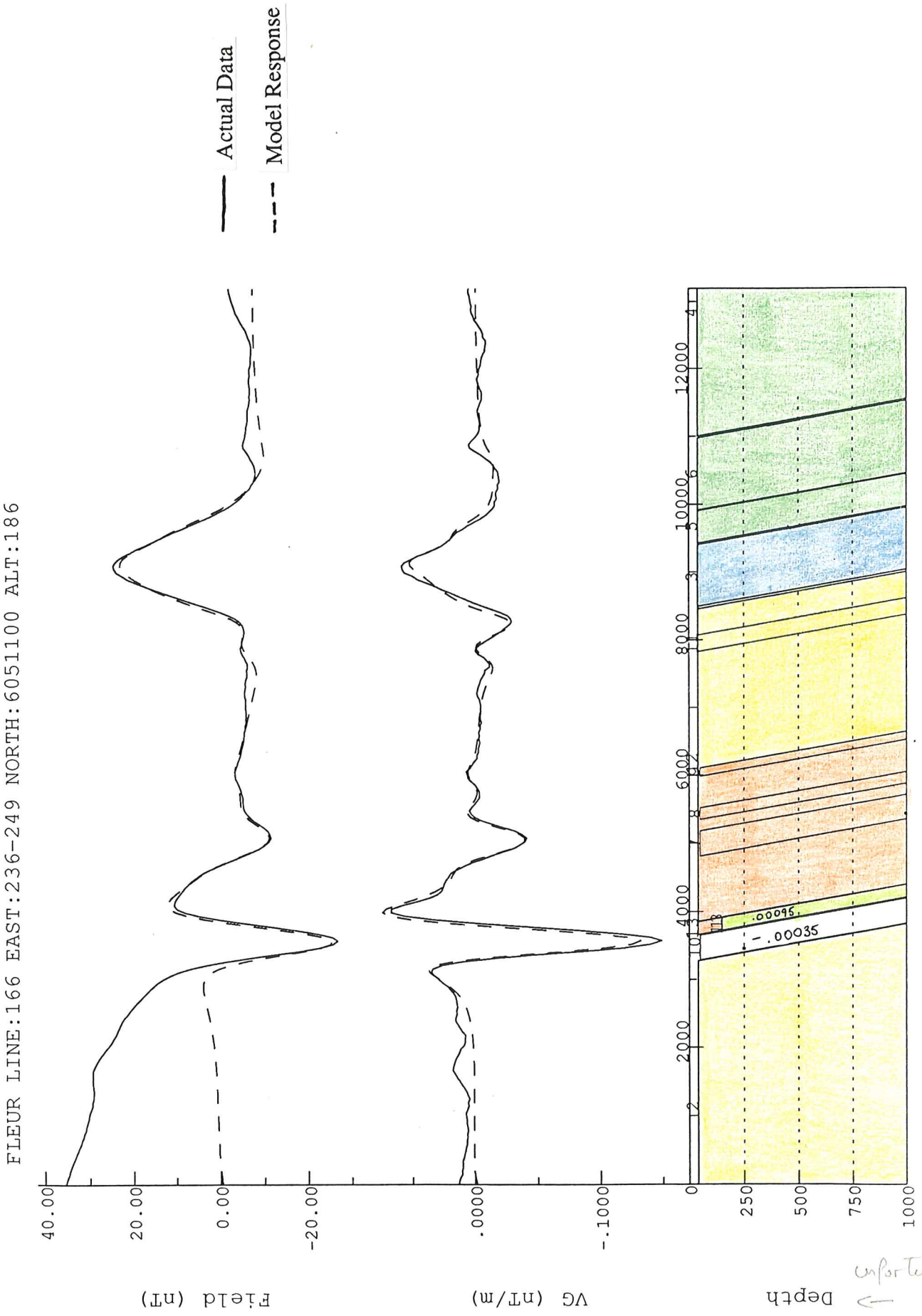

Figure 11: Line 166 data with model and model response. Total field and vertical gradient (VG) are shown.

4.3.2: Lines 182, 191 & 200

These lines all have very similar models even though the character of the profile anomaly changes markedly. The lines represent lines flown progressively northward and are spaced approximately 1km apart. In each case a smaller peak associated with the Talisker Formation can be seen to the east. This is modelled by a progressively-widening body with moderate susceptibility.

The magnetic source for the main peak corresponds to the position of the Ulupa Siltstone. Variation in the thickness of this body occurs between models (150-215m), but the modelled susceptibility (180×10^{-5} SI units) is relatively constant with values similar to those observed elsewhere.

A major feature of the models is the rocks that surround the magnetic source. These are modelled by large bodies with low susceptibilities (1×10^{-5}-50×10^{-5} SI) of the same order as expected for Kanmantoo Group rocks and their positions correspond with mapped rock boundaries (Fig. 3). Dips on all bodies in the models (65°-75°) correspond with the dip seen on the rock units in the Talisker area (60°-80°), and small negative susceptibilities on some of these modelled bodies suggests that the remnant component is present but, as previously discussed, is not overwhelming.

Local small anomalies can be modelled by magnetic bodies with slightly different susceptibilities than the main units. These changes are likely to represent slight, but real, susceptibility variations in the rocks due to the variable composition of layers within rock units.

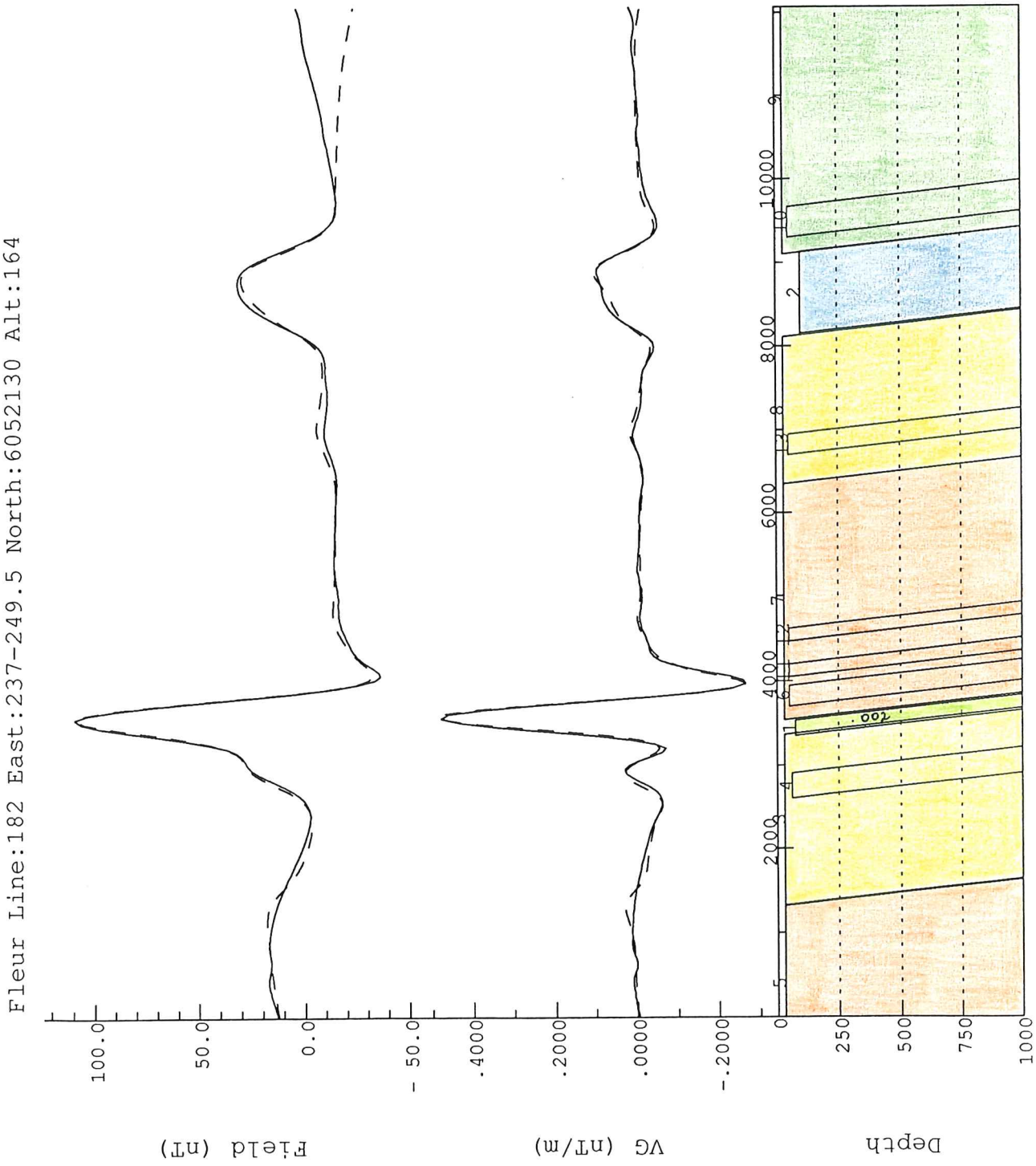

Figure 12: Line 182 data with model and model response. Total field and vertical gradient are shown.

Figure 13: Line 191 data with model and model response. Total field and vertical gradient are shown.

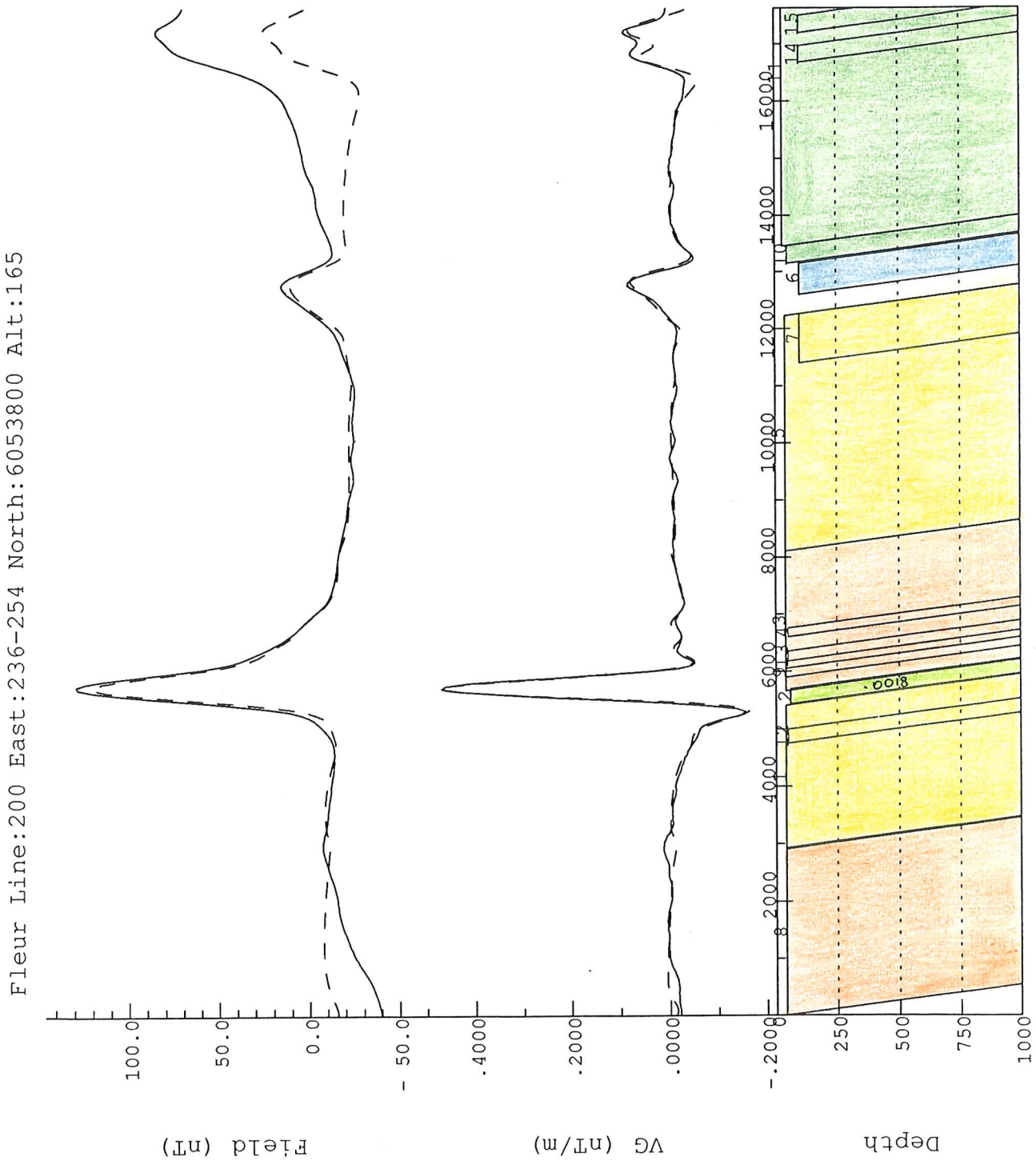

Figure 14: Line 200 data with model and model response. Total field and vertical gradient are shown.

4.3.3: Line 223

This is the northern most line that was modelled, and corresponds with the southerly edge of the Permian glacial cover. The data in this line appear very noisy due to the laterite seen here. Laterites tend to produce noisy data because of the random magnetization effects they produce.

It should be noted that the scale of the data in this modelled profile is different from previous models. GAMMA produces scales in its graphical representation of data that makes the data fit on an A4 sheet. Hence, the vertical scale for this profile is different from the previous models. This will also apparently amplify the smaller anomalies and the noise within the data. (To get a true representation of the data see the original profiles presented in Appendix Two.) The peak can still be modelled by a magnetic body consistent with the body seen in the previous models and consistent with the Ulupa Siltstone. The body associated with this anomaly, however, is at a greater depth than that modelled in the previous profiles, and is covered by non-magnetic material that masks the anomaly further. The top of the body here is at a depth of 250m compared to 60-100m in the other lines.

The second major feature of these data is the double peak appearance of the anomaly. This is modelled by a second body adjacent to the Ulupa Siltstone body, which has parameters similar to those described as Talisker Calc-siltstone in previous models. The geological map (Fig. 4) also show Talisker Formation in the vicinity of the Talisker Mine suggesting a major fault, between line 191 and line 223, which moves the Talisker Formation closer to the Ulupa Siltstone in this location. This fault most probably is a feature associated with the shear zone, and could be difficult to map. The lateritic and Permian cover in the region present a problem with mapping. The body modelled by the polygon P1 (Figure 15) represents a major synclinal feature within the Backstairs Passage Formation that noses out south of line 223. (Fig. 3)

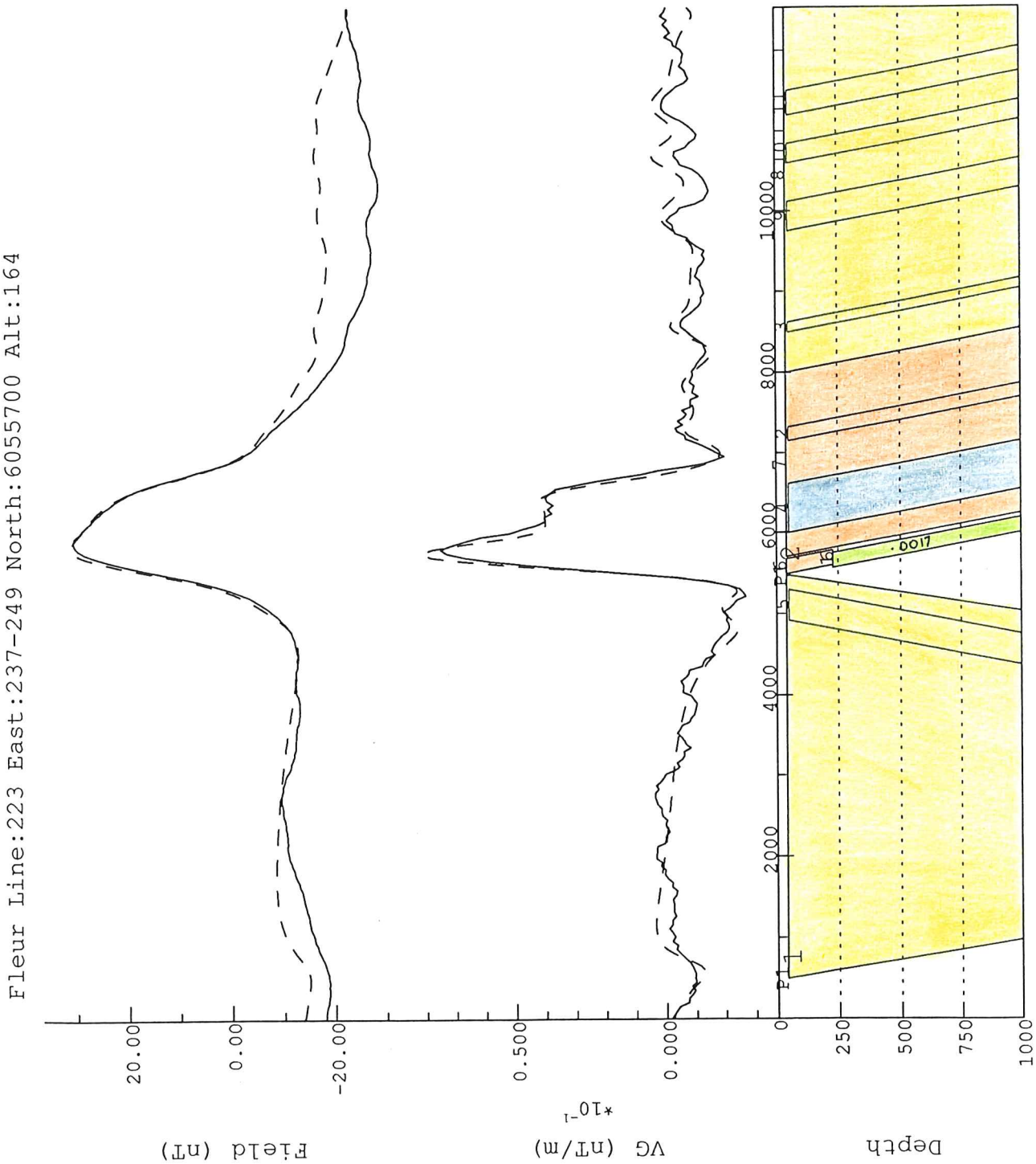

Figure 15: Line 223 data with model and model response. Total field and vertical gradient are shown.

4.4: Ground Traverses

The linear form of the main anomaly enabled ground magnetic traverses to be carried out across the strike of the anomaly to allow improved interpretation of the geology at depth. Several traverses were carried out between the mine site and the southern end of the anomaly to determine the position, characteristics, and strike variations of the magnetic body or bodies producing the anomaly. The position of these traverses can be seen on Figure 4. The models can be seen in Figures 16-20.

The traverses were located 200-300m apart to allow confident correlation between lines. Station spacings of 20m were used to enable long traverses to be completed quickly while still maintaining good resolution for modelling. Two short lines were also completed at 10m spacings to give greater accuracy over the magnetic bodies.

Base stations were located close to the position of the traverse, preferably near an easily-identifiable landmark. Repeat readings were made before and after each traverse and times noted. This enabled drift corrections to be made. Drift may introduce apparent anomalies in the data that are not due to variations in the magnetic properties of the rock units, and may be produced by low battery levels and variations in the solar magnetic cycle. If base readings are made at least every two hours, the drift can be assumed to be linear with time, and the data corrected accordingly. Correction for drift enables genuine variations in the Earth's magnetic field to be identified.

Ground profiles were carried out using a portable Barringer Research Ltd. GM-22 Proton Precession Magnetometer.

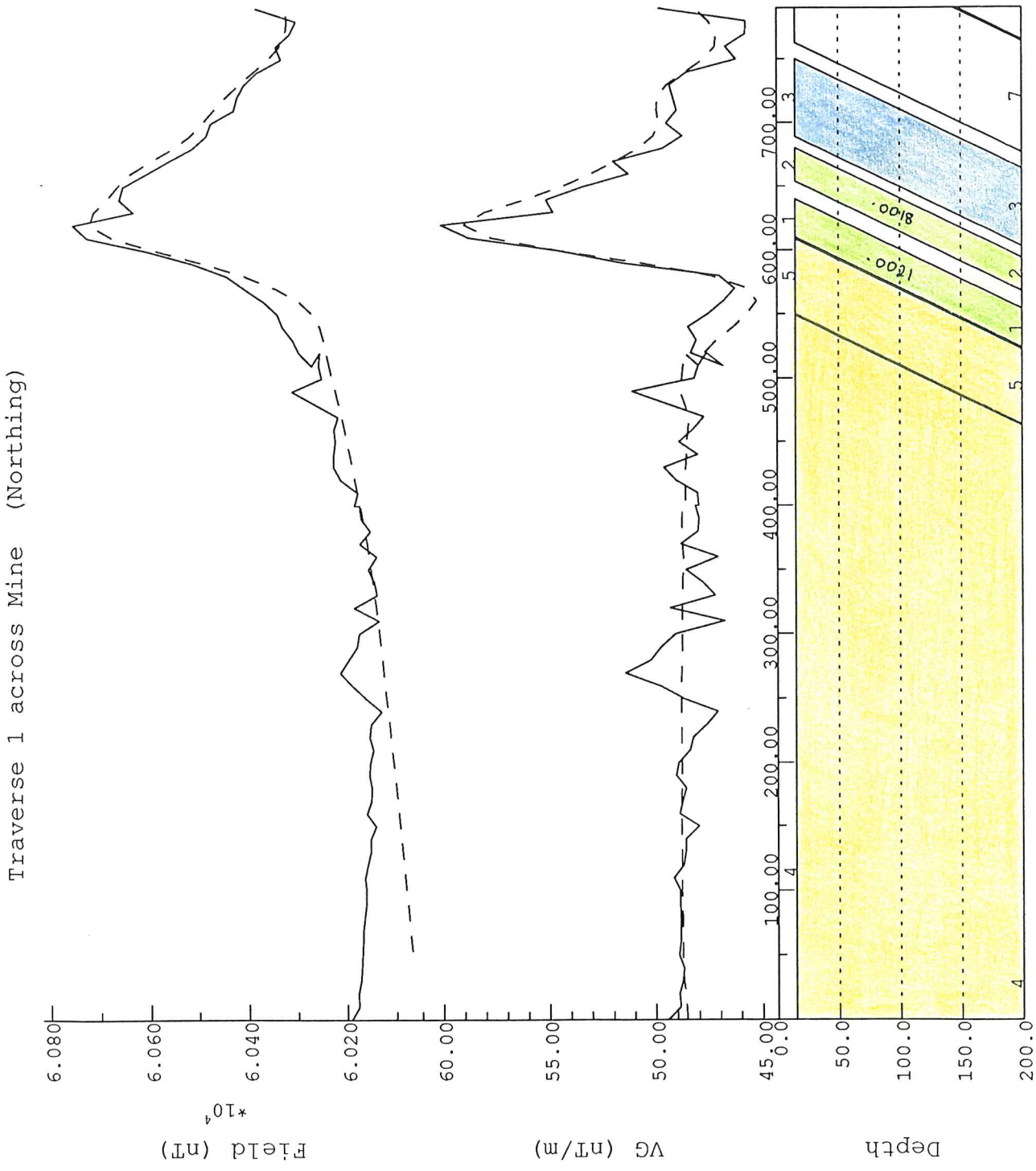

Figure 16: Ground magnetic traverse near mine site with data, model and model response. Total field and vertical gradient (VG) are shown.

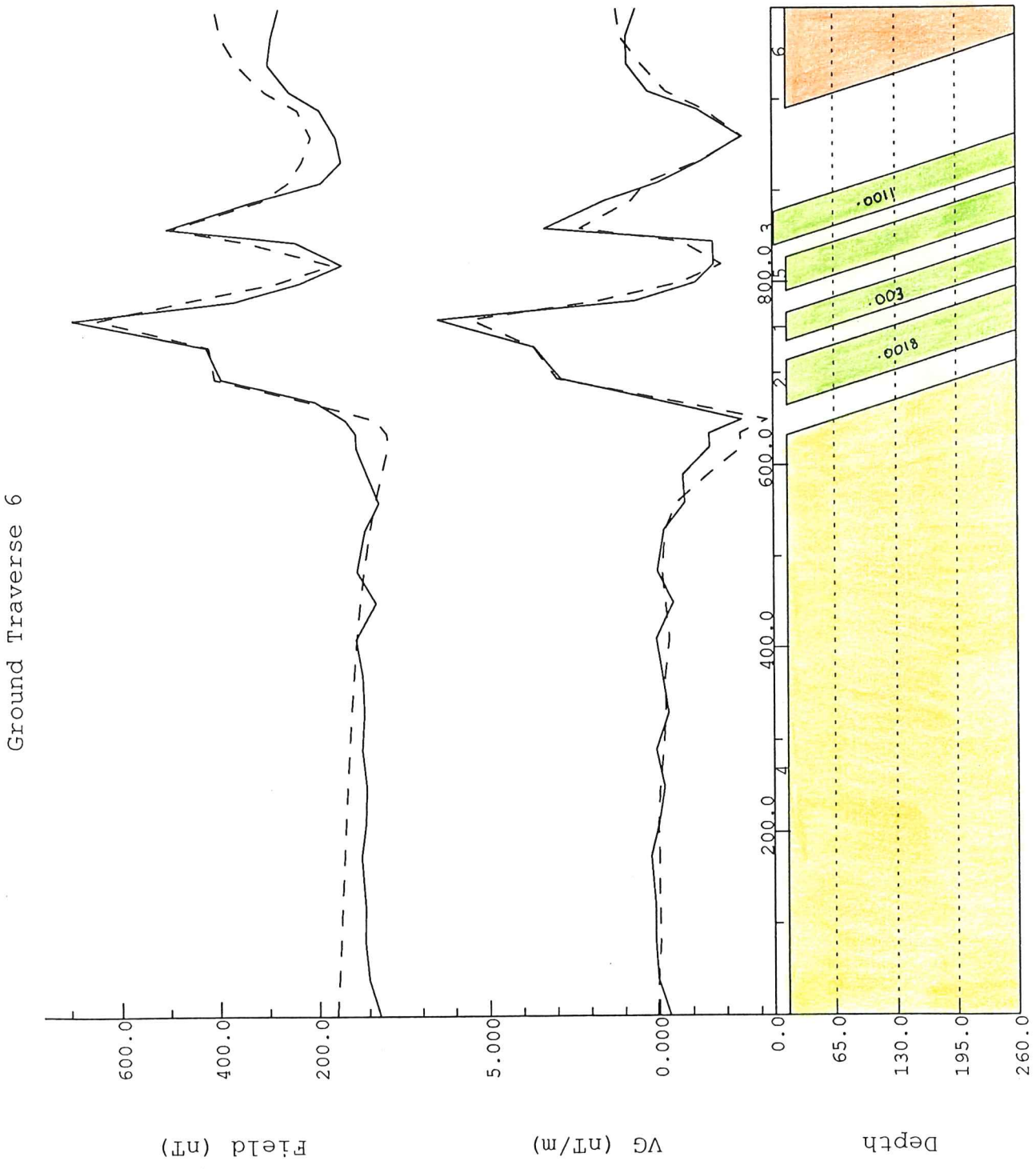

Figure 17: Ground magnetic traverse 6 with data, model and model response. Total field and vertical gradient are shown.

Figure 18: Ground magnetic traverse 7 with data, model and model response. Total field and vertical gradient are shown.

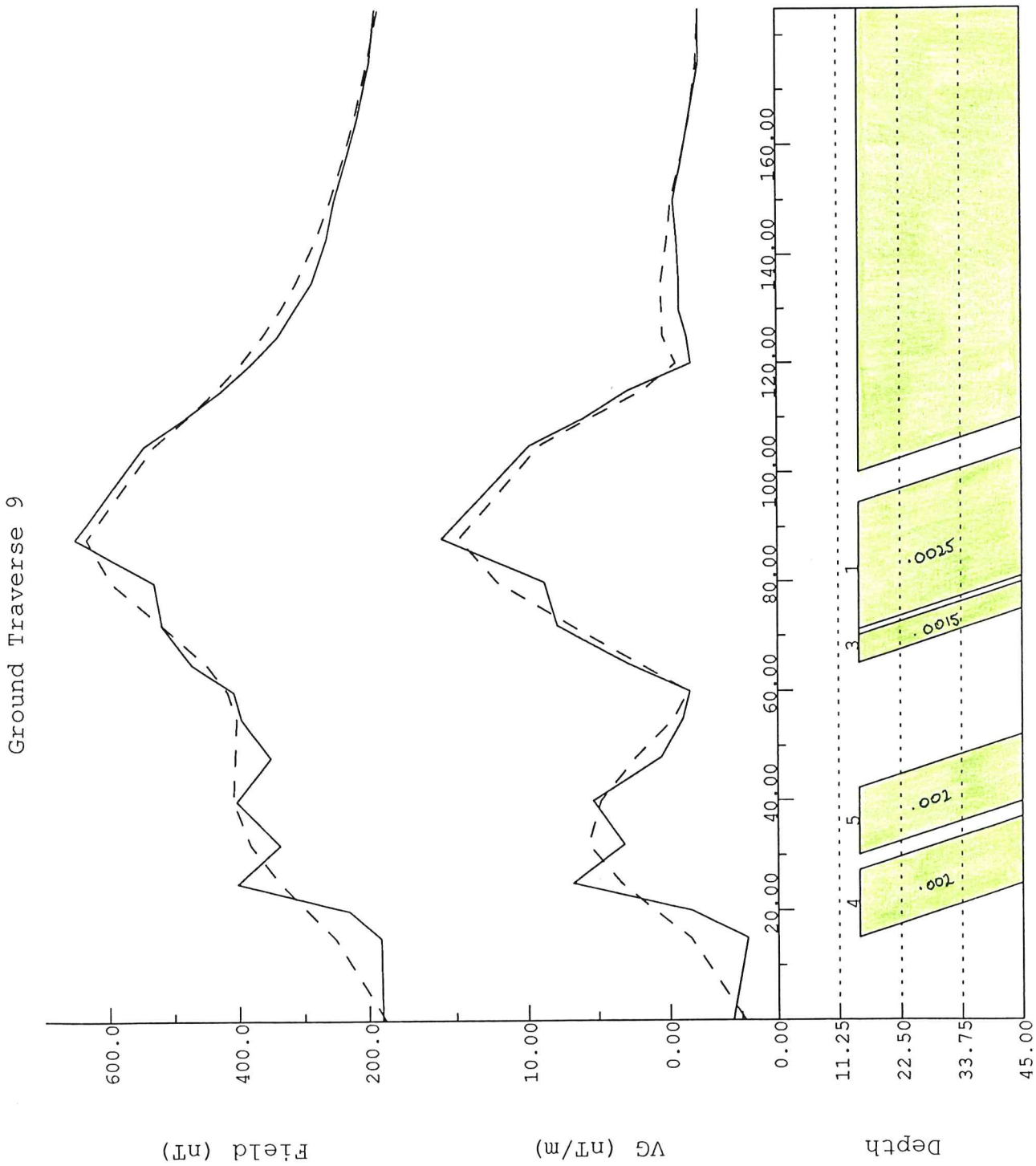

Figure 19: Ground magnetic traverse 9 with data, model and model response. Total field and vertical gradient are shown.

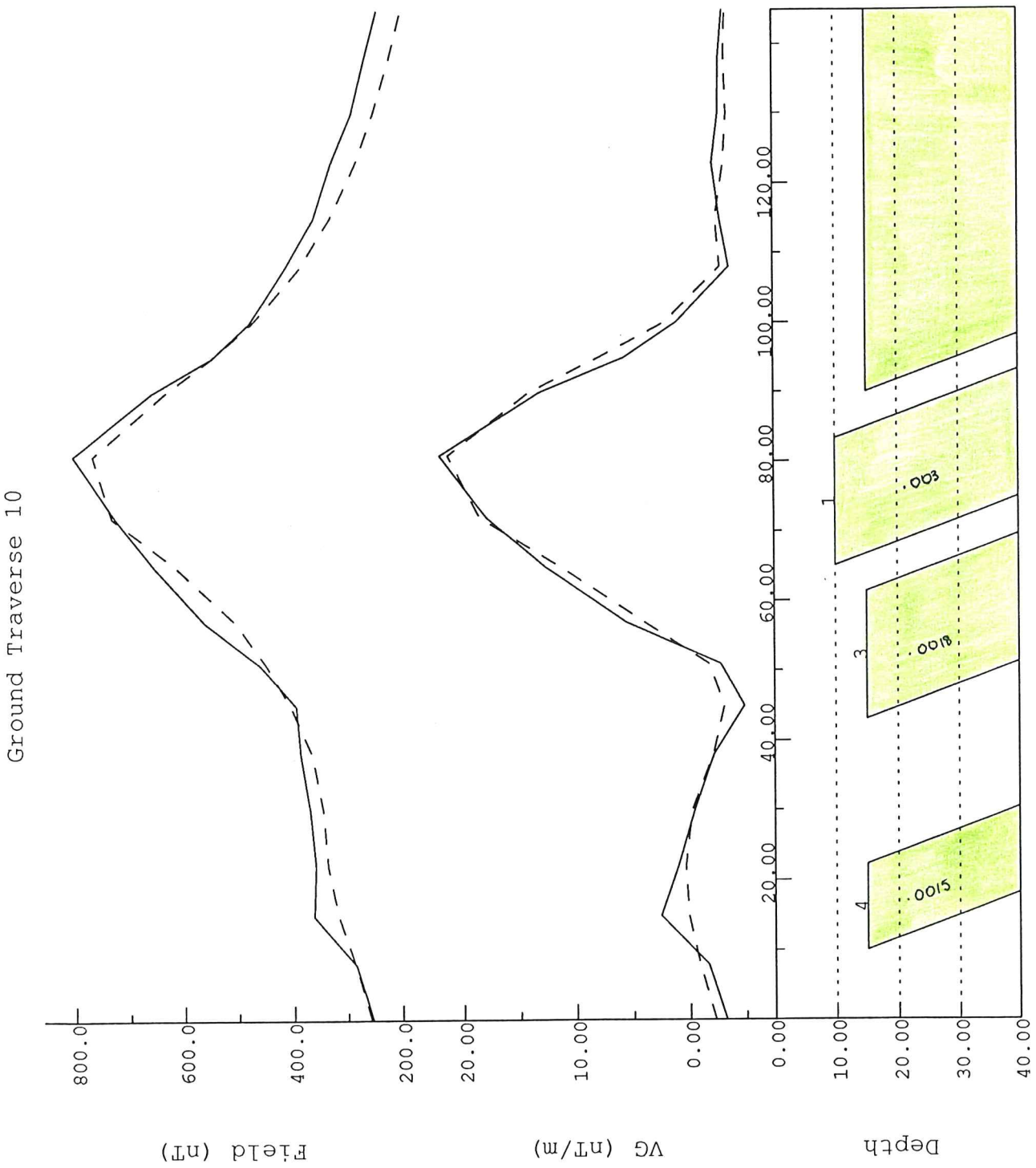

Figure 20: Ground magnetic traverse 10 with data, model and model response. Total field and vertical gradient are shown.

4.5: Modelling of Ground Magnetic Data

Ground traverse profiles have double peaks which may be modelled by two magnetic bodies with varying magnetic susceptibilities. Due to the apparently constant dip and strike of the beds in the Talisker area, all bodies were modelled with constant dip and strike. The bodies were modelled at shallow depths, indicating depths of weathering of 15m are present in this area.

Upward continuation to the aeromagnetic datum level was applied to two profiles revealing a single peak and amplitudes consistent with the air-borne data. However, the position of the peak in the upward continued data did not correspond to the position of the peak in the air-borne data, but corresponded to the peak position of the ground data.

As with the aeromagnetic data, the nature of the profiles show considerable variation. Large apparent differences in the profiles are partly due to the different scales produced by the Gamma plot. However, the profiles can be modelled with very similar models showing consistency along strike.

The magnetic bodies are surrounded by non-magnetic bodies that correspond to mapped boundaries of Kanmantoo Group rocks. Hence, they confirm the findings of the mapping.

Traverse 7 (Figure 18) has a different character from that seen in other profiles with only a single peak being observed. The profile is also modelled with only one body rather than two as in the other profiles. This profile corresponds with the position where the Ulupa Siltstone begins to tongue out and become sheared out against Backstairs Passage Formation rocks at the Talisker Fault. When the magnetic bodies are plotted on the geological map (Fig.4 overlay), it can be seen that the strike of the magnetic bodies is also consistent with them becoming sheared out along this western edge.

The profiles examined at Talisker have amplitudes and character similar to the ground traverses examined by Stolz (1985) at Delamere. Stolz (1985) also recognised the double peak feature in the anomalies at Delamere, but he recorded anomalies of the order of 1000nT. In the Talisker area, the anomalies observed were of the order of 600-800nT.

4.6: Discussion of Modelling

It is concluded from the modelling of the ground data at Talisker, that the Ulupa Siltstone in the Talisker area is a continuation of the body observed by Stolz (1985) at Delamere. However, the bodies become gradually sheared out against Backstairs Passage Formation in the Talisker area causing the magnetic anomaly to end south of the Talisker Mine.

The character and amplitudes of the anomalies at Delamere and the Talisker area are very similar, and the similarity in the models produced at both locations favours the interpretation that the anomalies at the two locations are caused by the same body. Stolz (1985) produced models having bodies with greater susceptibilities, but it is not unreasonable to expect slight susceptibility variations along strike. These susceptibility changes are suggested to be a true representation of magnetic mineral variations expected along strike.

CHAPTER 5: MINERALOGY AND PETROGENESIS

Polished thin sections were made from a representative sample of each rock unit mapped in the Talisker area. These were examined under transmitted and reflected light to study the amount and type of opaques present, and also to study the non-opaques (Figure 21).

5.1: Opaque Mineralogy

Samples from the Kanmantoo Group rocks contain minor amounts of opaques as accessory minerals which include pyrrhotite, haematite/rutile, ilmenite/haematite, and haematite/magnetite associations. However, the grain size of these opaques is very fine and amounts much less than 1% (visual estimation) were observed in all samples.

On examination, only one slide (920-1, Fig. 21a) was observed to have sufficient opaques to produce a sizable anomaly. This slide was observed to have up to 5% opaques and corresponded to the Ulupa Siltstone. Large euhedral porphyroblasts of magnetite were observed (Fig. 21b) which show characteristic martite texture. Martitization occurs as a result of weathering when magnetite becomes replaced by haematite along crystal cleavage boundaries. Haematite has low susceptibility and this indicates why lower-than-expected susceptibilities are observed in hand specimen.

Ilmenite/haematite associations are common in the andalusite schists of the Ulupa Siltstone in higher metamorphic grades (Rajagopalan, 1989). These associations can produce low susceptibilities in rocks with high percentages of opaque minerals. It is suggested by Rajagopalan (1989) that the exsolution blebs of ilmenite in haematite grains also indicates a possible cause for strong NRM in the Ulupa Siltstone. These associations are not observed in the Ulupa Siltstone sample from Talisker and it is concluded that the low measured susceptibilities are as a result of the martitization of magnetite in the weathered samples.

The Ulupa Siltstone also contains grains of rutile which have characteristic yellow internal reflection in polished section (Fig. 21c). Rutile and ilmenite are observed as occasional small inclusions within the large martitized grains of magnetite.

Occasional mottled grains are observed associated with the rutile and magnetite grains (Fig 21b). Confirmation of the identity of these grains was gained using the electron microprobe.

The dark phase of these mottled grains was identified as rutile, while the lighter patches were titaniferous magnetite (magnetite/ulvospinel).

Hence, the Ulupa Siltsone observed at Talisker contains abundant opaques consisting of large grains of martitized magnetite, and small grains of rutile, and titaniferous magnetite. Ulupa Siltstone sediments have been selectively enriched in titanium and are often also rich in iron and aluminium (Rajagopalan, 1989, Fig 22a).

Levels of titanium oxide for Ulupa Siltstone are characteristically 1-2%, while Kanmantoo Group rocks have levels usually less than 0.8% Titanium content is one of the characteristic differences between Ulupa Siltstone and Kanmantoo Group rocks. Whole rock analysis would enable titanium oxide contents to be determined allowing confident identification of the rock unit. Mancktelow (1979) collected a sample (Adelaide Uni. accession No. 474-121) from the mapped Ulupa Siltstone in the Talisker area which was examined and considered to be the rock type being analysed in this project. Whole rock analysis of this sample was carried out by Mancktelow (1979) and is summarized in Figure 22b. Levels of Titanium oxide of 1.09% were recorded giving a confident identification of Ulupa Siltstone.

Brotherton (1955; *in* Rajagopalan, 1989) showed oxidation ratios for the Ulupa Siltstone to be 55-60. This range of ratios and the amount of iron (shown to be 7-10% by Mancktelow (1979) and Rajagopalan (1989), Fig. 22) is consistent with magnetite formation during metamorphism. This probably formed from iron-bearing minerals deposited in the sediments.

The large size of the magnetite grains seen in hand specimen and thin section (Fig. 21b) compared to the grain size of the rock, indicates magnetite production occurred during metamorphism. Pressure shadows are also seen around magnetite grains (Fig. 21g-h) which suggests the magnetite was present before the shearing event.

a: Fine grained Ulupa Siltstone within the zone of shearing. Large euhedral porphyroblasts of magnetite are observed randomly in the fine mica-rich matrix. Other small opaque grains of rutile are observed.

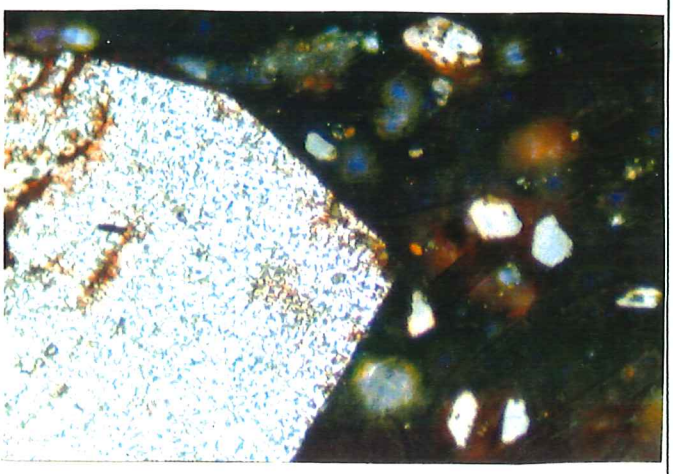

c: Ulupa Siltstone under reflected light (320x). Large magnetite grain (left) shows almost complete martitization to haematite. Smaller grains are rutile.

b: Ulupa Siltstone under reflected light (320x). Porphyroblasts of magnetite show martite texture (large grain on left). Rutile shows characteristic yellow internal reflection (middle). Mottled grains of rutile and titaniferous magnetite (right) are often seen.

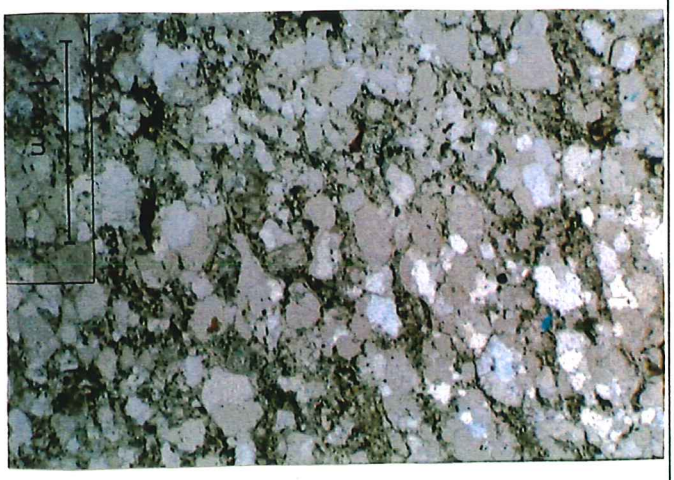

d: Unsheared Kanmantoo Group rock under transmitted light (analyser out). Quartz and feldspar grains make up the majority of the grains within a matrix of very fine-grained mica and quartz. Very few opaques are observed.

Figure 21: Photos of Ulupa Siltstone and Kanmnatoo Group rocks under transmitted and reflected light.

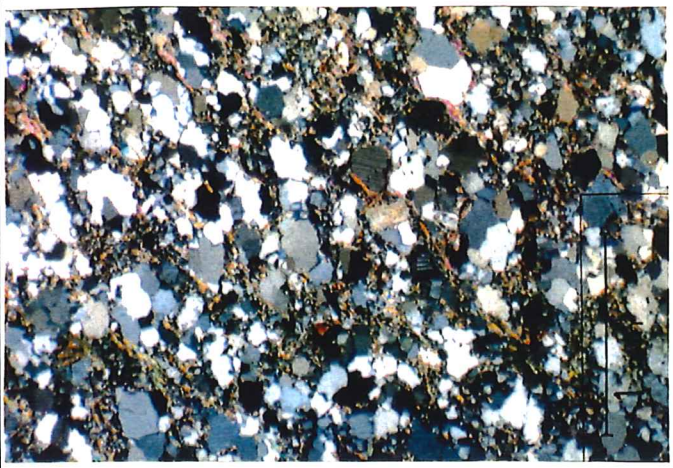

e: Previous slide with analyser in.

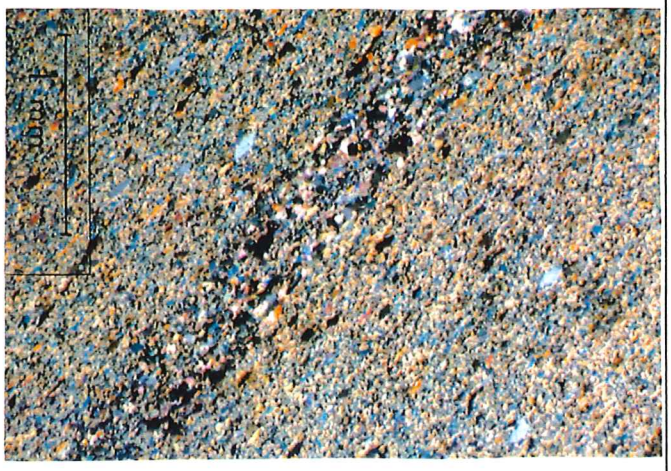

f: Talisker Calc-Siltstone within the zone of shearing under transmitted light (analyser in). Minor opaques are observed.

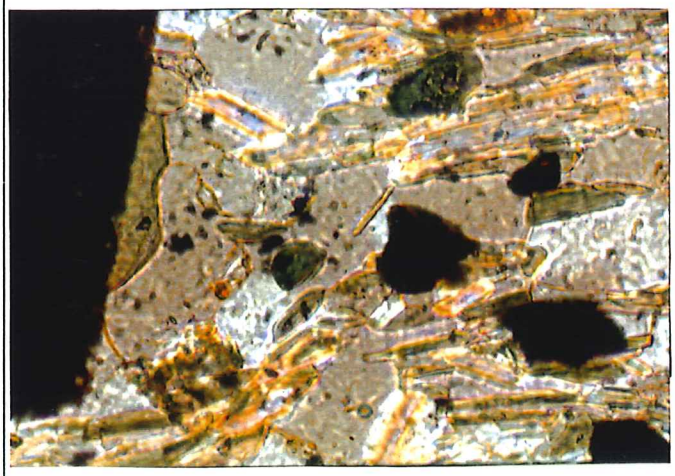

g: Ulupa Siltstone under transmitted light 320x (analyser out). Pressure shadows are observed behind the large magnetite porphyroblasts indicating they were present before shearing..

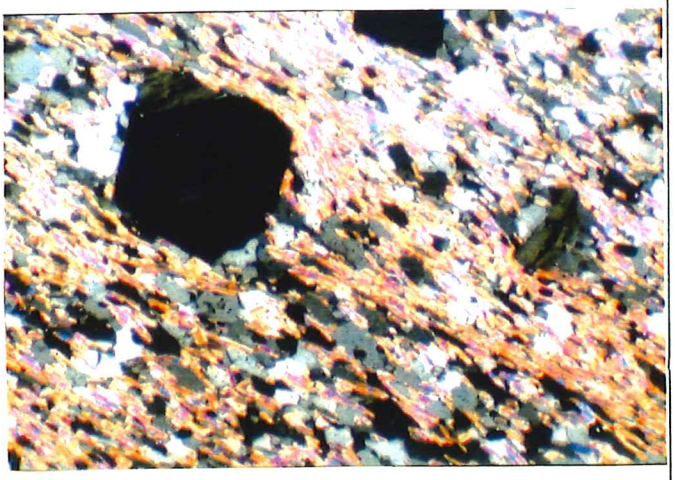

h: Ulupa Siltstone under transmitted light 32x (analyser in) shows pressure shadow behind magnetite porphyroblast.

	Brachina Subgroup	Carrickalinga Head	Backstairs Passage	Talisker	Tappanappa
SiO_2	61.07	62.88	74.75	55.82	62.73
Al_2O_3	16.76	16.12	11.83	15.80	16.20
Fe_2O_3	8.01	8.27	4.18	7.22	9.20
MnO	0.12	0.11	0.14	0.11	0.15
MgO	3.21	3.53	1.29	3.19	3.42
CaO	1.77	1.83	1.06	2.33	1.22
Na_2O	1.83	1.99	3.58	1.95	1.32
K_2O	3.61	3.03	2.17	3.28	4.40
TiO_2	1.20	0.74	0.43	0.65	0.74

Figure 22a Rock Mineralogy of Brachina Subgroup compared to Kanmantoo Group. (After Rajagopalan, 1989)

	Ulupa Siltstone	Kanmantoo Group
SiO_2	62.62	58.56
Al_2O_3	17.40	16.64
Fe_2O_3	7.21	6.67
MnO	0.05	0.09
MgO	2.49	5.10
CaO	0.59	3.38
Na_2O	0.95	2.39
K_2O	4.46	3.62
TiO_2	1.09	0.74

Figure 22b Whole Rock Analysis (After Mancktelow, 1979)

5.2: Non-Opaque Mineralogy

Fig 21 (a) shows Ulupa Siltstone under transmitted light. The very fine-grained nature of the rock, and its strong preferred cleavage, is highlighted by the predominance of mica in the specimen. Large grains of magnetite are observed randomly scattered throughout the section. Fine grains of quartz, biotite and muscovite make up the bulk of the matrix, with occasional grains of chlorite and amphibole. The predominantly fine-grained texture of the sample is characteristic of the sheared nature of the rock unit.

The Kanmantoo Group rocks (Figs 21c-21f) are predominantly quartz, biotite, muscovite, plagioclase and K-feldspar. The Talisker Calc-siltstone sample (Fig.21f) also contains bands of calcite. The unsheared rocks (Fig. 21d-e) are generally medium to fine grained, with equidimensional, sub-angular grains of quartz and feldspar in a very fine-grained mica-quartz-rich matrix. However, the highly sheared samples have much higher mica percentages, and the rocks are much finer grained (Fig. 21f). Whole rock analysis of these samples (as done by Mancktelow, 1979) show levels of Titanium oxide of 0.8%, characteristic of Kanmantoo Group rocks and lower than Ulupa Siltstone values.

The mineralogy indicates that the Ulupa Siltstone has sufficient magnetic, opaque minerals present to produce the anomaly seen in the Talisker area. The presence of large amounts of magnetite produces a large induction component in the magnetic response. The minor amounts of magnetite/ulvospinel produces only a slight remnance component and hence, the anomaly produced by these rocks will be dominated by the induction component.

CHAPTER 6: CONCLUSION

Evidence gathered in this project shows consistency with values of susceptibility and rock mineralogy expected for Ulupa Siltstone. The anomaly observed over the Talisker area is of the same order of magnitude as seen over the magnetic Brachina Formation at Delamere, and susceptibilities used in the modelling of magnetic profiles are appropriate for Ulupa Siltstone. Good curve matches are seen between sections of the observed anomalies and the models, which have characteristic Ulupa Siltstone values. Models also have consistency with the mapped boundaries of the magnetic Ulupa Siltstone.

Modelling of both aeromagnetic data and ground magnetic data show internal consistency along strike from profile to profile, even though the character of the anomalies changes slightly. These changes in character represent slight variation in the magnetic properties of the rocks along strike, which is to be expected. Modelling shows the Ulupa Siltstone to be a continuous body that is a continuation of the body producing the anomaly at Delamere. The apparent gap in the anomaly can be modelled by a body at greater depth than seen in the Talisker area. This correlates with the extensive Permian cover seen north of the Talisker area and may represent deeper weathering and a non-magnetic cover. More detailed mapping would be required to resolve this issue. The lateritic cover seen to the south of the Permian sediments also produces a masking effect and increases the amount of noise in the signal.

Microscopic mineralogy of the magnetic rock unit is consistent with the values expected for Ulupa Siltstone. Levels of Titanium, and the mineral assemblages are similar to those observed for Ulupa Siltstone elsewhere. The low remnant magnetization effect in the Talisker area may be explained by large amounts of magnetite and minor titaniferous magnetite observed in thin sections. This results in an anomaly that is dominated by the induction effect.

Mapping has shown the Ulupa Siltstone to exist as a tongue of rock within a zone of intense deformation. The Ulupa Siltstone becomes sheared out along the western boundary of this zone against unsheared Backstairs Passage Formation rocks. The end of the anomaly corresponds to the end of the mapped Ulupa Siltstone and further suggests that Ulupa Siltstone is causing the anomaly. Further mapping will reveal the extent of the shear zone in this area.

A reasonable model for the Ulupa Siltstone was deduced in the Talisker area and it is highly likely that magnetic Ulupa Siltstone is the cause of the magnetic anomaly observed over the Talisker area on the Southern Fleurieu Peninsula.

REFERENCES

Both, R.A., (In press)

Geology and Mineral Deposits of the Kanmantoo Trough.

In Geology of the Mineral Deposits of Australia & Papua-New Guinea

ed. F.E. Hughes J. Australasian Inst. Min. & Metall.

Campana, B. & Wilson, B., (1954)

Jervis Map Sheet Geological Atlas of South Australia, 1:63,360 Series

Geological Survey of South Australia.

Daily, B. & Milnes, A.R., (1971).

Stratigraphic notes on Lower Cambrian Metasediments between Campbell Ck. and Tunkalilla Beach in the type section of the Kanmantoo Group, Fleurieu Peninsula, South Australia.

Trans. R. Soc. S. Aust. *95(4)*:199-214.

Daily, B. & Milnes, A.R., (1972).

Revision of the Stratigraphic Nomenclature of the Cambrian Kanmantoo Group, South Australia.

J. Geol. Soc. Aust. *19(2)*:197-202.

Daily, B. & Milnes, A.R., (1973).

Stratigraphy,Structure and Metamorphism of the Kanmantoo (Cambrian) in its Type Section East of Tunkalilla Beach, South Australia.

Trans. R. Soc. S. Aust. *97(3)*:213-242.

Dalgarno, R., (1983).

GSA Abstracts No. 10.

Dobrin, M.B., (1981).

Introduction to Geophysical Prospecting.

McGraw Hill International Book Company, New York.

George, R.J., (1963).

The Geology of the Talisker Mine Area.

Hons Thesis, University of Adelaide (unpubl).

James, P.R., (1989).

Field Excursion Guide. Structural Geology of the Fleurieu Peninsula.

Notes of the Australasian Tectonics Conference.

Geol. Soc. Aust.

Jenkins, R.J.F. (1986).

Ralph Tate's Enigma-And the Regional Significance of Thrust Faulting in the Mt. Lofty Ranges.

Eighth Australian Geol. Convention. G.S.A. Abstracts 15, 101.

Mancktelow, N.S., (1979).

The Structure and Metamorphism of the Southern Adelaide Fold Belt.

Ph.D. Thesis, University of Adelaide (unpubl).

Offler, R. & Fleming, P.D., (1968).

A Synthesis of Folding and Metamorphism in the Mt. Lofty Ranges, South Australia.

Geol. Soc. Austr. *15(2)*:245-266.

Preiss, W.V. (compiler) (1987).

The Adelaide Geosyncline. Late Proterozoic Stratigraphy, Sedimentation, Palaeontology and Tectonics.

Bulletin 53, Geological Survey of South Australia.

Plummer, P.S., (1978).

Stratigraphy of the Lower Wilpena Group (late Precambrian), Flinders Ranges, South Aust.

Trans. R. Soc. of South Australia *102(1&2)*:25-38.

Rajagopalan, S. (1989).

Aeromagnetic Interpretation of the Kanmantoo Group, South Aust.

Ph.D. Thesis, University of Adelaide (unpubl).

SADME (1989).

Oil, Gas & Coal Division, Petroleum Exploration & Development in S.A.

Pg 92-98.

Stacey, F.D. & Banerjee, S.K. (1974).

The physical Principles of Rock Magnetism.

Elsevier Scientific Publishing Company, Amsterdam.

Stolz, E.M. (1985).

A Magnetics Study of the Brachina Formation on Southern Fleurieu Peninsula, South Australia.

Honours Thesis, University of Adelaide (unpubl.).

Steinhardt, C. (in press).

Thrusting and the Tectonic Development of the Adelaide Geosyncline.

Submitted to Tectonics.

Thomson, B.P., Daily, B., Coats, R.P., Forbes, B.G., (1976).

Excursion Guide No. 33A

25th International Geological Congress. Pg 14.

BIBLIOGRAPHY

Boyd, D., (1967).

The Contribution of Airborne Magnetic Surveys to Geological Mapping.

Mining and Groundwater Geophysics. pp213-227.

McIntyre, J.I., (1980).

Geological Significance of Magnetic Patterns Related to Magnetite in Sediments and Metasediments - A Review.

Bull. Aust. Soc. Expl. Geophys. *11(1/2)*:19-31.

Nixon, L.G.B., (1938)

Talisker Lead-Arsenic Mine.

Mining Review *108*:22-31.

Nixon, L.G.B., (1938)

Talisker Lead-Arsenic Mine. Second Report.

Mining Review *108*:32-56.

APPENDIX ONE

TABLE: MODELLING SUMMARY

Date: 10/8/89 Sheet: Line: 166

Field Intensity: 60,000 nT Inclination: -67.5° Declination: 7°

BODY NUMBER	Position m	Depth m	Strike °	Suscept. S.I.	Dip °	Depth Extent m	Width m	Index Parame
1	3728.8	150	35	0.00095	65	1000	150	
2	-996.5	40	35	0.00005	65	1000	3500	
3	8453.5	40	35	0.00016	65	1000	780	
4	11000	40	35	-0.00003	65	1000	3000	
5	9428.3	40	35	0.00003	65	1000	400	
6	9900	40	35	-0.00005	65	1000	880	
7	4804	50	35	-0.0001	65	1000	300	
8	5339	50	35	0.00008	65	1000	140	
9	5984	50	35	0.00006	65	1000	100	
10	3289	50	35	-0.00035	65	1000	300	
11	7823	40	35	0.00007	65	1000	200	
12	3854	40	35	-0.00002	65	1000	150	

TABLE: MODELLING SUMMARY

Date: 1/8/89 Sheet: Line: 182

Field Intensity: 60,000nT Inclination: -67.5° Declination: 7°

BODY NUMBER	Position m	Depth m	Strike °	Suscept. S.I.	Dip °	Depth Extent m	Width m	Index Parame
1	3350	75	35	0.002	75	1000	150	
2	8150	100	35	0.0001	75	1000	800	
3	1320	30	35	0.00005	75	1000	1675	
4	2600	60	35	0.00027	75	1000	250	
5	-520	30	35	0.00015	75	1000	1500	
6	3700	50	35	-0.0009	75	1000	200	
7	3540	30	35	-0.0001	75	1000	2300	
8	6350	30	35	-0.00007	75	1000	1440	
9	9100	30	35	-0.00015	75	1000	3000	
10	9300	50	35	-0.00007	75	1000	300	
11	4050	50	35	0.00008	75	1000	120	
12	4460	50	35	0.00008	75	1000	125	
13	6700	50	35	0.00005	75	1000	200	

TABLE: MODELLING SUMMARY

Date: 2/8/89 Sheet: Line: 191

Field Intensity: 60,000nT Inclination: -67.5° Declination: 7°

BODY NUMBER	Position m	Depth m	Strike °	Suscept. S.I.	Dip °	Depth Extent m	Width m	Index Parame
1	2004.3	40	35	0.0001	75	1000	2000	
2	4480.66	75	35	0.0018	75	1000	215	
3	4761.13	40	35	-0.0001	75	1000	2000	
4	5200	40	35	0.00018	75	1000	125	
5	7500	40	35	-0.00014	75	1000	2845	
6	10675	100	35	0.00001	75	1000	700	
7	9222.5	100	35	0.00008	75	1000	300	
8	2	40	35	0.00008	75	1000	1650	
9	5002	40	35	-0.0002	75	1000	125	
10	11952	50	35	-0.00007	75	1000	250	
11	11532	30	35	-0.00012	75	1000	2000	
12	3803	50	35	0.0001	75	1000	200	

TABLE: MODELLING SUMMARY

Date: 9/8/89 Sheet: Line: 200

Field Intensity: 60,000 nT Inclination: -67.5° Declination: 7°

BODY NUMBER	Position m	Depth m	Strike °	Suscept. S.I.	Dip °	Depth Extent m	Width m	Index Parame
1	2909	40	35	0.00008	65	1000	2050	
2	5440	60	35	0.0018	65	1000	215	
3	5665	40	35	-0.0001	65	1000	2000	
4	6600	50	35	0.00018	65	1000	125	
5	8105	40	35	-0.00014	65	1000	3375	
6	12600	100	35	0.00005	65	1000	450	
7	11400	100	35	0.00004	65	1000	700	
8	-0.5	40	35	0.00005	65	1000	2400	
9	5900	40	35	-0.0002	65	1000	125	
10	13150	50	35	-0.0003	65	1000	250	
11	13450	30	35	-0.00012	65	1000	5000	
12	4750	50	35	0.00007	65	1000	200	
13	6180	50	35	0.00025	65	1000	140	
14	16675	100	35	0.00054	65	1000	235	
15	17200	100	35	0.00045	65	1000	250	

TABLE: MODELLING SUMMARY

Date: 11/8/89 Sheet: Line: 223

Field Intensity: 60,000 nT Inclination: -67.5° Declination: 7°

BODY NUMBER	Position m	Depth m	Strike °	Suscept. S.I.	Dip °	Depth Extent m	Width m	Index Parame
1	5562	230	35	0.0017	65	1000	150	
2	7147	50	35	0.00005	65	1000	140	
3	8500	50	35	0.00006	65	1000	100	
4	6000	50	35	0.00014	65	1000	500	
5	4920	50	35	0.00005	65	1000	310	
6	5490	40	35	-0.00001	65	1000	150	
7	5700	40	35	-0.00005	65	1000	1885	
8	8000	40	35	-0.00008	65	1000	4000	
9	9750	50	35	0.00002	65	1000	300	
10	10600	50	35	0.00003	65	1000	200	
11	11200	50	35	0.00002	65	1000	250	
$P1_1$	500	40	35	0.00004				
$P1_2$	4080	0						
$P1_3$	3700	1000						
$P1_4$	405	1000						

TABLE: MODELLING SUMMARY

Date: 8/9/89 Sheet: Line: Mine Traverse

Field Intensity: 60,000 nT Inclination: -67.5° Declination: 7°

BODY NUMBER	Position m	Depth m	Strike °	Suscept. S.I.	Dip °	Depth Extent m	Width m	Index Parame
1	640	15	35	0.0021	75	1000	18	
2	680	15	35	0.0018	75	1000	15	
3	750	15	35	0.0006	75	1000	35	
4	550	15	35	-0.0009	75	1000	500	
5	610	15	35	-0.0015	75	1000	35	
6	1200	15	35	0.0003	75	1000	200	
7	850	15	35	-0.0003	75	1000	50	

TABLE: MODELLING SUMMARY

Date: 4/9/89 Sheet: Line: Traverse 6

Field Intensity: 60,000nT Inclination: -67.5° Declination: 7°

BODY NUMBER	Position m	Depth m	Strike °	Suscept. S.I.	Dip °	Depth Extent m	Width m	Index Parame
1	735	15	35	0.003	75	1000	25	
2	665	15	35	0.0018	75	1000	40	
3	840	2	35	0.0011	75	1000	30	
4	-100	15	35	-0.0001	75	1000	600	
5	790	15	35	-0.00055	75	1000	30	
6	990	15	35	0.0007	75	1000	100	

TABLE: MODELLING SUMMARY

Date: 4/9/89 Sheet: Line: Traverse 7

Field Intensity: 60,000 nT Inclination: -67.5° Declination: 7°

BODY NUMBER	Position m	Depth m	Strike °	Suscept. S.I.	Dip °	Depth Extent m	Width m	Index Parame
1	-100	15	35	-0.00006	75	1000	400	
2	475	15	35	0.0018	75	1000	25	

TABLE: MODELLING SUMMARY

Date: 19/9/89 Sheet: Line: Traverse 9

Field Intensity: 60,000 nT Inclination: -67.5° Declination: 7°

BODY NUMBER	Position m	Depth m	Strike °	Suscept. S.I.	Dip °	Depth Extent m	Width m	Index Parame
1	70	15	35	0.0025	75	1000	20	
2	100	15	35	-0.0007	75	1000	500	
3	65	15	35	0.0015	75	1000	5	
4	15	15	35	0.002	75	1000	10	
5	30	15	35	0.002	75	1000	10	

TABLE: MODELLING SUMMARY

Date: 20/9/89 Sheet: Line: Traverse 10

Field Intensity: 60,000 nT Inclination: -67.5° Declination: 7°

BODY NUMBER	Position m	Depth m	Strike °	Suscept. S.I.	Dip °	Depth Extent m	Width m	Index Parame
1	65	10	35	0.003	75	1000	15	
2	90	15	35	-0.0008	75	1000	100	
3	43	15	35	0.0018	75	1000	15	
4	10	15	35	0.0015	75	1000	10	

APPENDIX TWO

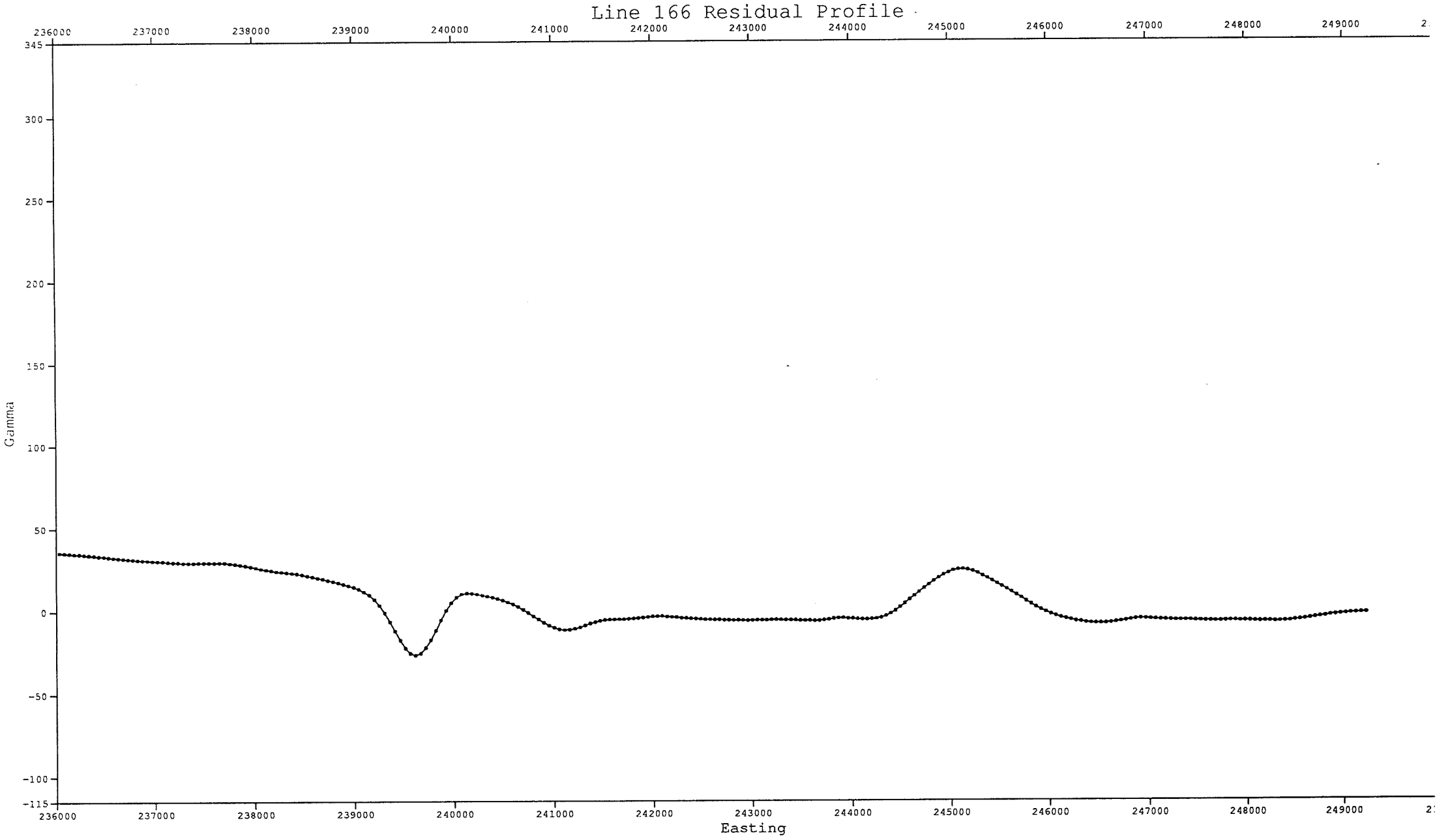
Line 166 Residual Profile
236000
237000
238000
239000
240000
241000
242000
243000
244000
245000
246000
247000
248000
249000
345
300
250
200
150
100
50
0
-50
-100
-115
Gamma
Easting

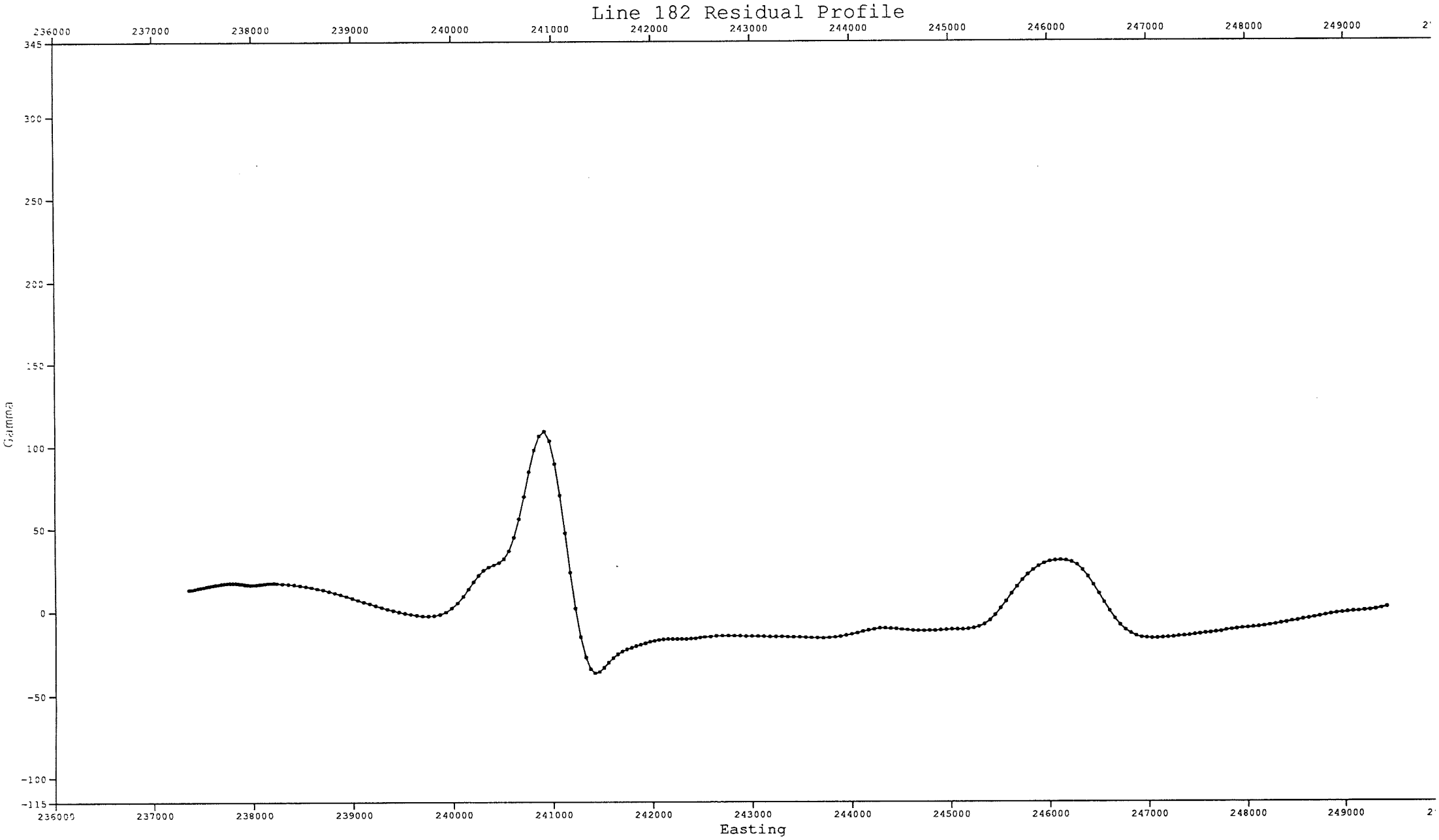
Line 182 Residual Profile
236000
237000
238000
239000
240000
241000
242000
243000
244000
245000
246000
247000
248000
249000
345
300
250
200
150
100
50
0
-50
-100
-115
Gamma
Easting

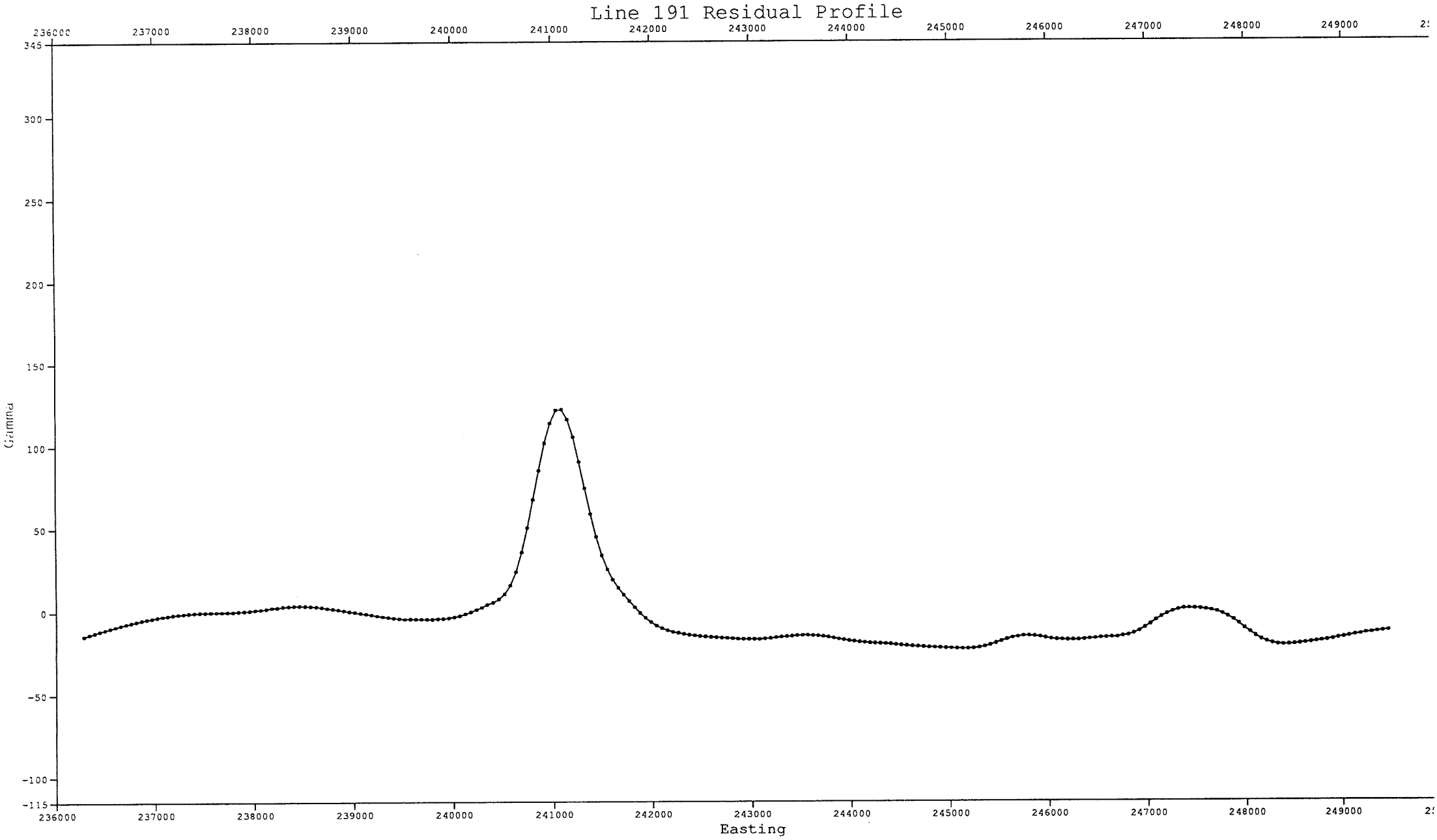
Line 191 Residual Profile
236000
237000
238000
239000
240000
241000
242000
243000
244000
245000
246000
247000
248000
249000
345
300
250
200
150
100
50
0
-50
-100
-115
Gamma
Easting

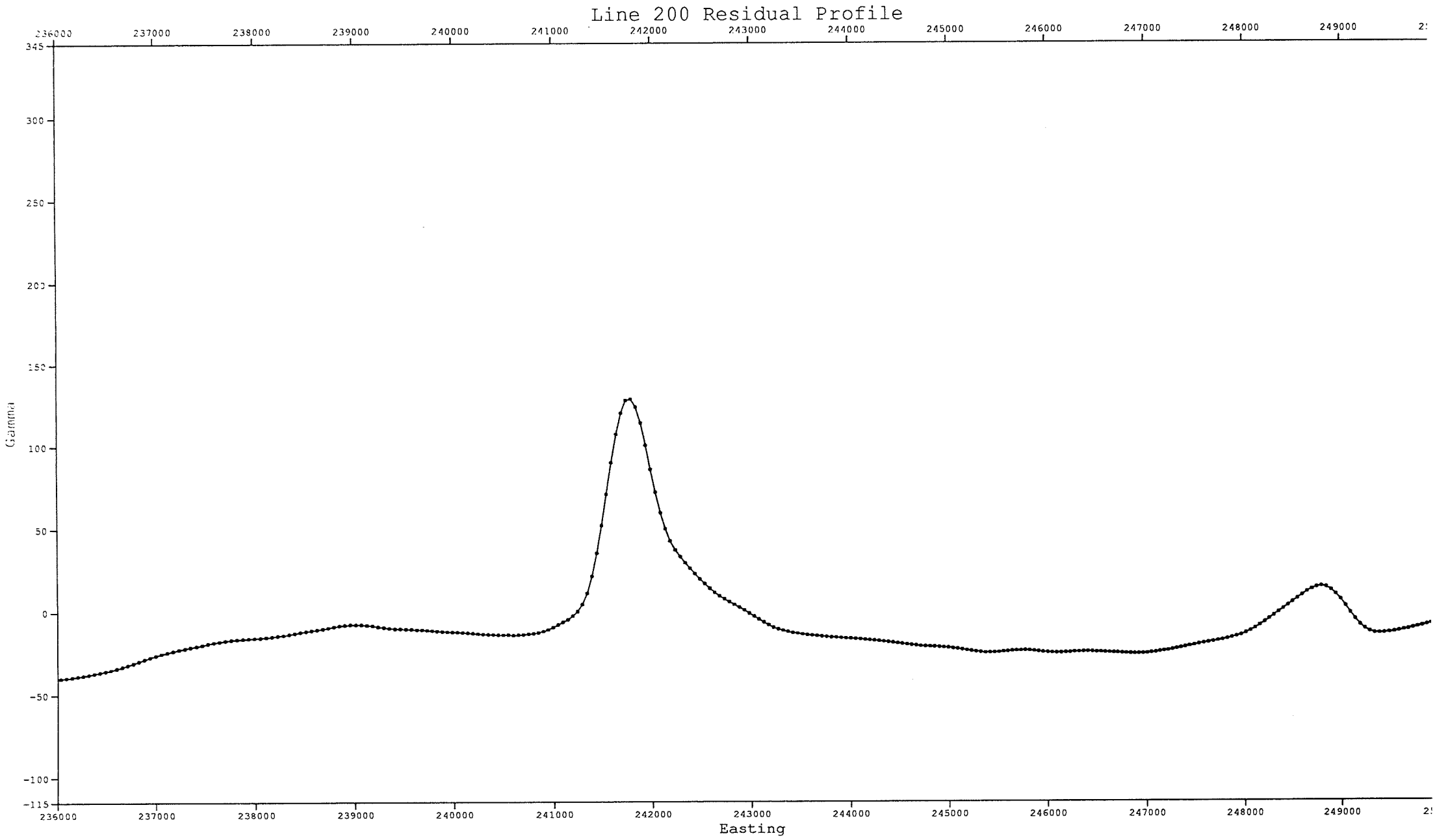
Line 200 Residual Profile
236000
237000
238000
239000
240000
241000
242000
243000
244000
245000
246000
247000
248000
249000
345
300
250
200
150
100
50
0
-50
-100
-115
Gamma
Easting

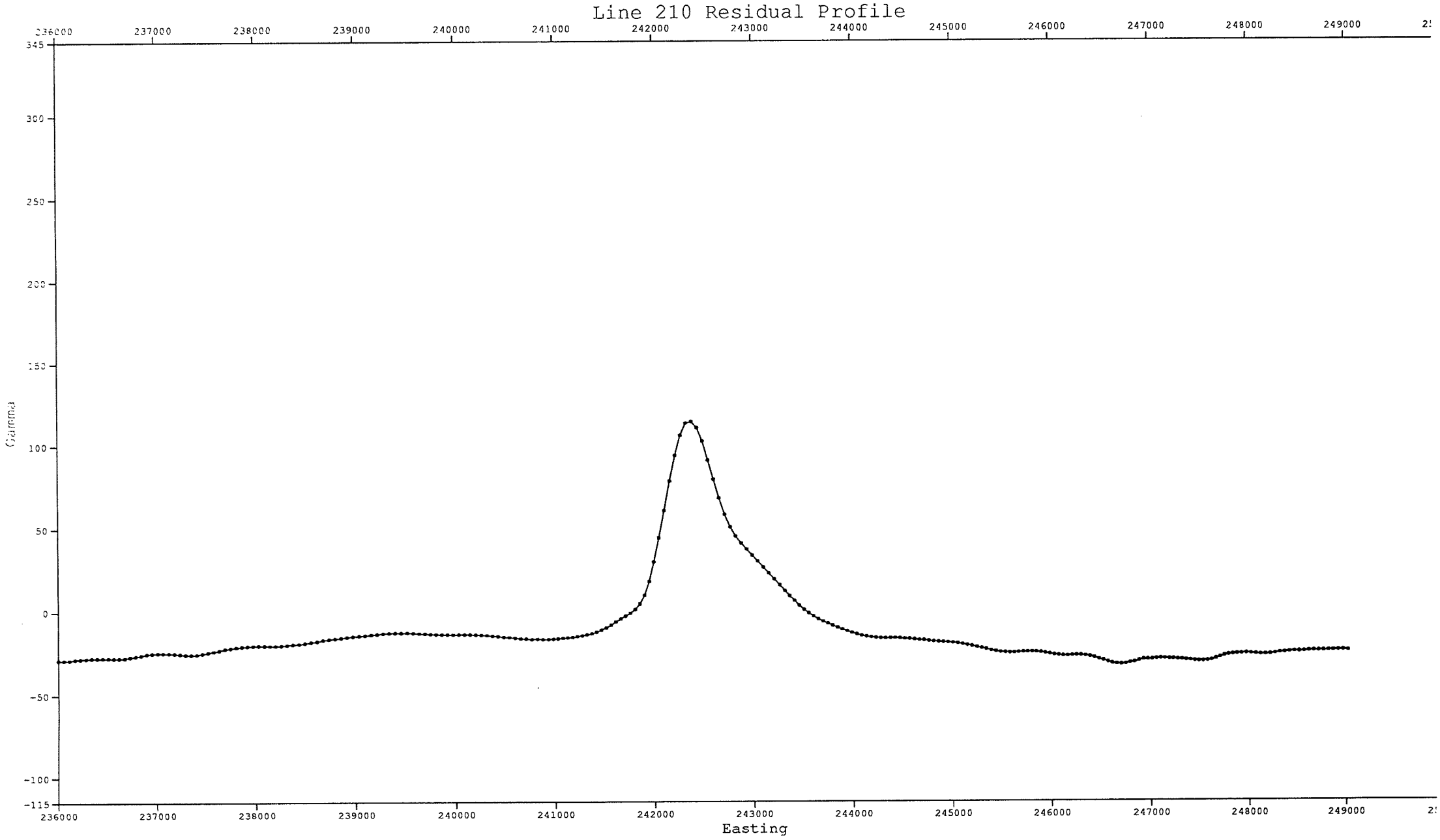
Line 210 Residual Profile
236000
237000
238000
239000
240000
241000
242000
243000
244000
245000
246000
247000
248000
249000
345
300
250
200
150
100
50
0
-50
-100
-115
Gamma
Easting

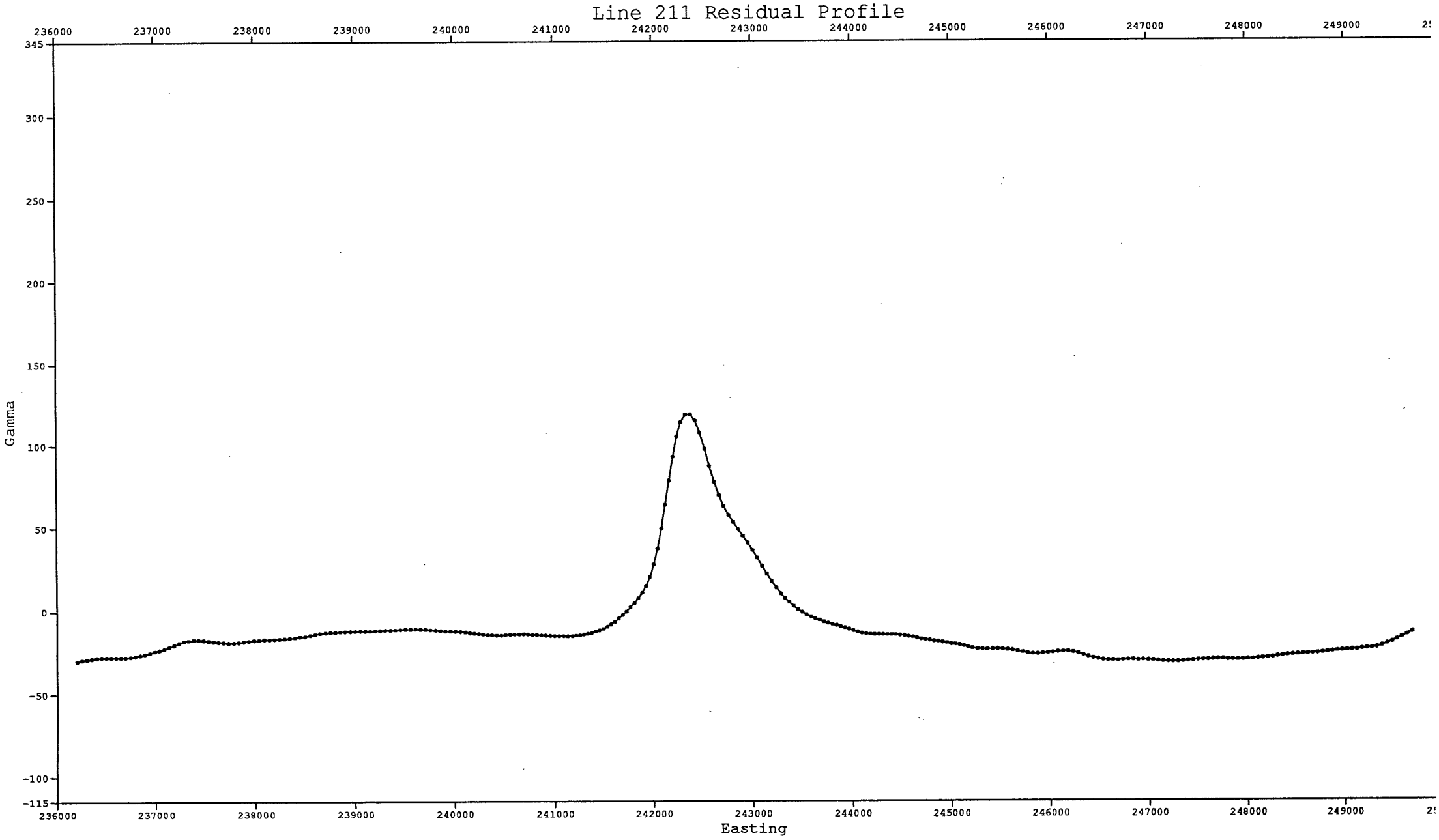
Line 211 Residual Profile
236000
237000
238000
239000
240000
241000
242000
243000
244000
245000
246000
247000
248000
249000
345
300
250
200
150
100
50
0
-50
-100
-115
Gamma
Easting

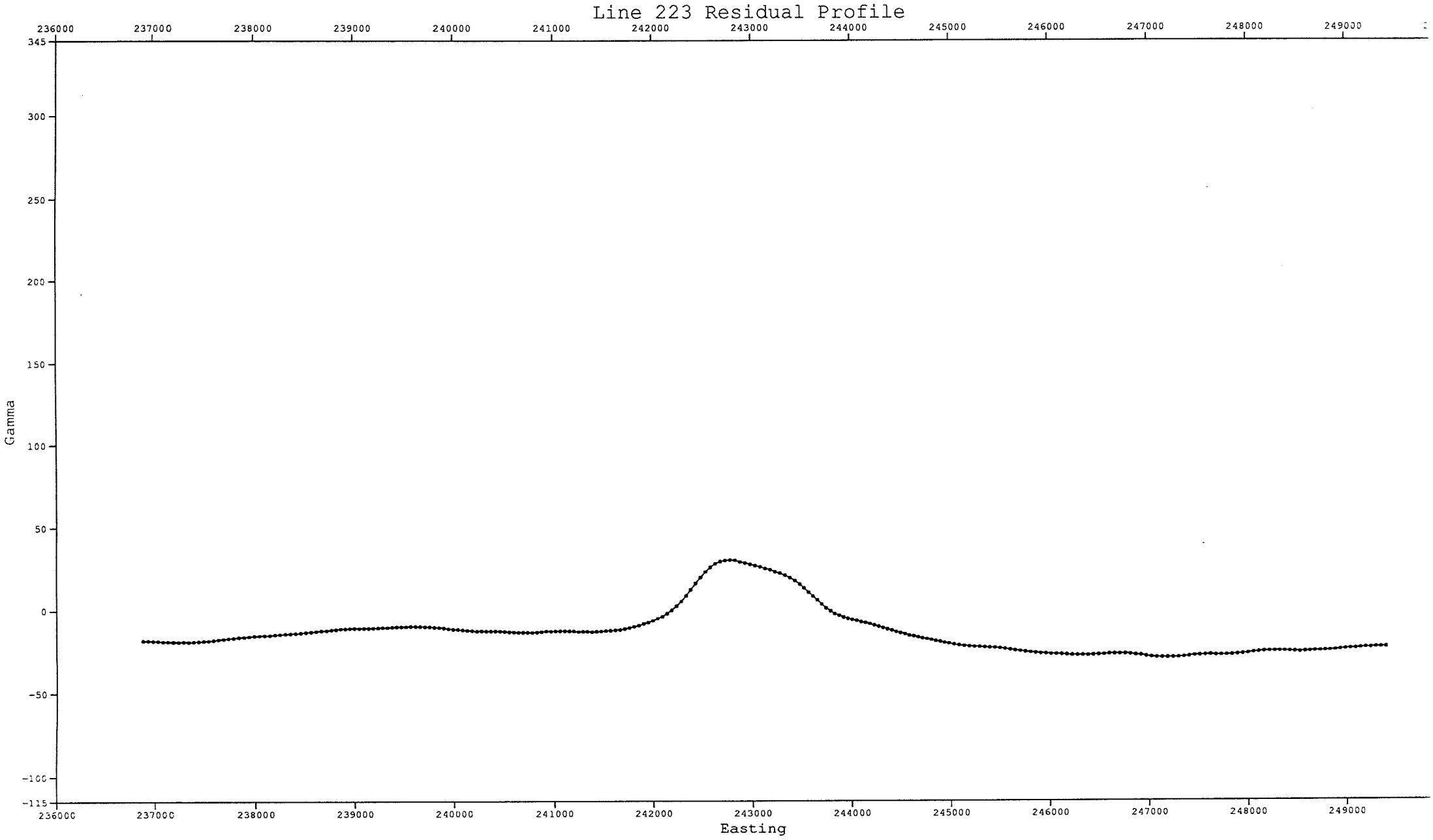
Line 223 Residual Profile
236000
237000
238000
239000
240000
241000
242000
243000
244000
245000
246000
247000
248000
249000
345
300
250
200
150
100
50
0
-50
-100
-115
Gamma
Easting